Phosphorylation and stabilization
of yeast zinc ion transporter Zrg17
by the endoplasmic reticulum-stress sensor Ire1
小胞体ストレスセンサーIre1 による酵母亜鉛輸送体
Zrg17 によるリン酸化と安定化

Nguyen Sy Le Thanh

Laboratory of Molecular and Cell Genetics
Nara Institute of Science and Technology
Graduate School of Biological Sciences
(Prof. Kohno Kenji)

2013/08/07

Graduate School of Biological Sciences　Doctoral Thesis Abstract

Lab name (Supervisor)	Laboratory of Molecular and Cell Genetics (Prof. Kenji Kohno)		
Name (surname) (given name)	Nguyen Sy Le Thanh	Date	2013/07/08
Title	Phosphorylation and stabilization of yeast zinc ion transporter Zrg17 by the endoplasmic reticulum-stress sensor Ire1		

Abstract

　　Zinc ions are known to function as an essential cofactor not only for a large number of cytosolic or nuclear proteins but also for various luminal and secretory proteins. Therefore, proper distribution of zinc ions between cytosol/nuclei and membrane-bound cellular compartments may be an important issue especially in case of zinc deficiency. Indeed, zinc deficiency causes endoplasmic-reticulum (ER) stress, which in yeast *Saccharomyces cerevisiae* cells, is aggravated by deletion of the *ZRG17* gene encoding an ER-membrane-located zinc-ion transporter. Here I have approached relationship between zinc depletion (and intracellular zinc-ion transporter Zrg17) and ER stress (and ER-stress sensor Ire1) in yeast cells.

　　According to immunopurification of epitope-tagged Ire1 from yeast cell lysates and mass-spectrometric identification of co-purified proteins, my current laboratory previously suggested that Zrg17 is one of the possible Ire1-interacting proteins. Ire1 is an ER-located transmembrane protein conserved among eukaryotic cells. The luminal domain of Ire1 captures ER-accumulated unfolded proteins, triggering the unfolded protein response (UPR). I have started my study from confirmation of co-immunoprecipitation of influenza hemagglutinin (HA)-epitope tagged Ire1 (Ire1-HA) and Myc-tagged Zrg17 (Zrg17-Myc). Although a luminal-domain partial-deletion mutation (the ΔIII mutation) of Ire1 abolishes interaction between Ire1 and ER-accumulated unfolded proteins, ΔIII Ire1 was associated with Zrg17-Myc as well as wild-type Ire1-HA. It is thus unlikely that Zrg17-Myc is captured by Ire1-HA merely as an unfolded protein that evokes the UPR. Rather I think that the interaction between Zrg17 and Ire1 implies a new molecular-biological event.

　　The cellular amount of Zrg17-Myc decreased upon culturing yeast cells in moderately zinc depletion conditions (at 30 °C in low-zinc medium (LZM) supplemented with 10 μM $ZnCl_2$ for 10 hrs). When the cells were then shifted to LZM not supplemented with $ZnCl_2$, the cellular level of Zrg17-Myc increased within 3 hrs.

This is partially due to transcriptional induction, as Zrg17-Myc is expressed from the *ZRG17* promoter, which is upregulated by cytosolic zinc depletion. Nevertheless, the Zrg17 induction was also controlled in another fashion in which Ire1 is involved. This is because *ire1Δ* cells showed the induction of Zrg17-Myc similarly to wild-type *IRE1* cells at the transcriptional level, but only poorly as for the protein level. A cycloheximide-chase experiment exhibited that Ire1 acts to stabilize Zrg17-Myc.

Ire1 has Ser/Thr kinase and endoribonuclease (RNase) motifs on its cytosolic domain. It is widely known that upon ER stress, Ire1 is autophosphorylated and then functions as an RNase to splice the *HAC1* mRNA, the spliced product of which is translated to a transcription factor protein that induces the UPR. However, here I noticed that for the induction (stabilization) of Zrg17-Myc, Ire1 functions in a different manner. The *hac1Δ* mutant did not compromise the Zrg17-Myc induction. Moreover, an RNase-activity-deficient mutant Ire1, but not a kinase-activity-deficient mutant, functioned to induce Zrg17-Myc. I thus think that Ire1 acts as a kinase to stabilize Zrg17. Indeed, Phos-tag-containing-acrylamide electrophoresis indicated that Zrg17 is phosphorylated dependently on Ire1. Considering transcriptional induction of the *ZAP1* gene, Zrg17 and Ire1 leads to depletion of cytosolic/nuclear zinc ions upon severe zinc deficiency. I thus think that under the severe zinc deficient condition, Ire1 stabilizes Zrg17 causing efficient cytosol-to-ER zinc transport.

In addition, I have asked how zinc deficiency leads to ER stress. ΔIII Ire1, which cannot capture ER-accumulated unfolded proteins, is known to exhibit wild-type-like activation upon membrane-lipid aberrancy but to be poorly activated by accumulation of unfolded proteins. Thus it is likely that ER accumulation of unfolded proteins and membrane-lipid aberrancy are different types of ER stress that activate Ire1 in different manners. Because the ΔIII mutation compromised Ire1's activity upon zinc deficiency, I think that at least partly, zinc depletion damages the ER through inhibition of protein folding in the ER.

Taken together, here I propose a new function of Ire1 controlling zinc-ion distribution in yeast cells upon zinc deficiency. When zinc deficiency is moderate, Zrg17 is destabilized, and zinc-ion homeostasis in cytosol and the nuclei is maintained. However, severe zinc deficiency inhibits protein folding in the ER and strongly activates Ire1, causing phosphorylation and stabilization of Zrg17. Thus a limited amount of zinc ions are properly distrusted between the ER and cytosol/nuclei.

List of Publications

Lab name (Supervisor)	Molecular and Cell Genetics (Prof. Kenji Kohno)		
Name (surname) (given name)	Nguyen Sy Le Thanh	Date	(2013/0707/)

First-author publication(s) from your doctoral research
  (Title, authors, year of issue, name of the journal, volume, page)

Zinc Depletion Activates the Endoplasmic Reticulum-Stress Sensor Ire1 via Pleiotropic Mechanisms. Nguyen TS, Kohno K, Kimata Y. Biosci Biotechnol Biochem. 2013, 77(6), 1337-1339.

Other co-authored publication(s) during your doctoral research
  (Title, authors, year of issue, name of the journal, volume, page)

Cloning, high-level expression, purification, and properties of a novel endo-beta-1,4-mannanase from *Bacillus subtilis* G1 in *Pichia pastoris*. Vu TT, Quyen DT, Dao TT, Nguyen Sle T. J Microbiol Biotechnol. 2012 Mar; 22(3):331-338.

TABLE OF CONTENTS

LIST OF FIGURES

LIST OF TABLES

I. INTRODUCTION

The endoplasmic reticulum (ER) is a membrane-bound cellular compartment in which newly-born secretory proteins are folded. Moreover, enzymatic reactions for membrane-lipid biosynthesis occur on the ER. Dysfunction or damage to the ER, namely ER stress, often accompanies production and accumulation of unfolded proteins in the ER. Eukaryotic cells cumulatively evoke a protective response, namely the unfolded protein response (UPR), against ER stress. The UPR is known as transcriptional induction of a variety of genes, mainly those encoding proteins that work in and on the ER. Ellis *et al.* (2004) reported that zinc deficiency causes the UPR in yeast and mammalian cells.

Zinc ions are an essential nutrient for all living organisms. A number of proteins require zinc ions as a functional and structural cofactor. Although the most well-known example might be zinc-finger transcription factors, which work in the nuclei, zinc ions are also required by various secretory proteins, such as insulin. It is thus possible that zinc depletion can impair protein folding in the ER. Existence of diverse intracellular transporters for zinc ions (Eide, 2006) implies importance of zinc ions in various cellular compartments.

The mechanism by which ER accumulation of unfolded proteins leads to the UPR is well-documented (Ron and Walter, 2007; Mori 2009). Ire1, an evolutionarily conserved eukaryotic type-I transmembrane protein located on the ER, serves as a trigger of the UPR. Upon accumulation of unfolded proteins in the ER, Ire1 molecules are self-associated to forms high-order homo-oligomers, which can be seen fluorescence-microscopically as punctate spots by using the GFP-tagging or the immunofluorescent staining techniques (Kimata *et al.*, 2007;

Aragon *et al.*, 2009; Li *et al.*, 2010). When homo-associated, the luminal domain of Ire1 forms a groove-like structure which may be able to capture unfolded proteins (Credle *et al.*, 2005). Two research groups have reported that Ire1 strongly shows its enzymatic activities noted in the next paragraph when physically interacting to ER-accumulated unfolded proteins (Kimata *et al.*, 2007; Gardner and Walter, 2011).

The cytosolic domain of Ire1 has dual enzymatic motifs, Ser/Thr protein kinase and endoribonuclease (RNase; Mori *et al.*, 1993; Shamu and Walter, 1996; Sidrauski and Walter, 1997). The kinase activity of Ire1 is known to contribute to *trans*-autophosphorylation, which means that an Ire1 molecule phosphorylates a neighboring Ire1 molecule in an oligomer (Shamu and Walter, 1996). X-ray crystal structure of the cytosolic domain of Ire1 clearly demonstrated that at least in the case of wild-type Ire1, its aotophosphorylation is a prerequisite for evocation of the RNase activity (Lee et al., 2008). Ire1-dependent UPR is due to splicing of mRNAs encoding transcription factor proteins, *Saccharomyces cerevisiae* (hereafter called simply yeast) Hac1 and metazoan XBP1 (Cox and Walter 1996; Yoshida *et al.*, 2001; Calfon *et al.*; 2002). Only after splicing by Ire1, these mRNAs are translated into functional transcription factors that induce gene expression for the UPR. In metazoan cells, Ire1 also promotes degradation of mRNAs encoding secretory proteins (Hollien and Weissman, 2006; Hollien *et al.*, 2009; Han *et al.*, 2009). This event may contribute to alleviation of ER stress through reduction of protein load in the ER. In these cases, Ire1 works on target molecules as an RNase, and its kinase activity is not absolutely required (Papa et al., 2003). Indeed, yeast Ire1 carrying the D828A or the D797N/K799N point mutation is able to evoke the UPR, though these mutations are likely to abolish Ire1's kinase activity (Chawla *et al.*, 2011; Rubio *et al.*, 2011).

It is likely that disturbance of membrane-lipid homeostasis is

another type of ER-stressing stimulus which is sensed by Ire1 in a manner that is different from interaction of unfolded proteins to Ire1. According to Promlek *et al.* (2011), yeast Ire1 carrying a mutation impairing the physical interaction between Ire1 and unfolded proteins (the ΔIII mutation; deletion of a.a. 253-272) was activated as well as wild-type Ire1 when cells were stressed by inositol depletion or deletions of genes related to lipid metabolism or intracellular lipid transport. On the other hand, the ΔIII mutation compromised activation of Ire1 upon accumulation of unfolded proteins in the ER (Kimata *et al.*, 2007, Promlek *et al.*, 2011). Moreover, Volmer *et al.* (2013) showed that recombinant Ire1 fragments not carrying the unfolded-protein-capturing region are autophosphorylated on chemically-synthesized liposomes dependently on lipid composition of the liposomes. It is thus likely that Ire1 *per se* monitor membrane-lipid integrity through an uncovered mechanism. Activation of Ire1 and evocation of the UPR by membrane-lipid aberrancy seems physiologically meaningful, since the UPR target genes include not only those encoding ER-located molecular chaperones and protein-folding enzymes but also those encoding factors for membrane-lipid biosynthesis and transport (Travers *et al.*, 2000; Kimata *et al.*, 2006).

My study bases on a preliminary research performed by my current laboratory. In order to find novel aspects of function and regulation of Ire1, T. Tsutsumi performed anti-hemagglutinin (HA) epitope immunopurification of HA-tagged Ire1 (Ire1-HA) from yeast cells carrying a multi-copy (2μ) Ire1-HA (Kimata *et al.*, 2003), and identified co-purified proteins using the mass spectrometry technique. One of the resulting Ire1-interactor candidates, Zrg17, is a multiple membrane-spanning protein belonging to the cation diffusion facilitator (CDF) family of metal ion transporters. As its name denotes (Zinc Regulated Genes), Zrg17 is induced upon zinc deficiency, at least at the mRNA level (Lyons *et al.*, 2000; Yuan, 2000). Zrg17 is located on the ER (Ellis *et al.*, 2005).

Zrg17 forms a heterocomplex with another ER-located CDF-family protein Msc2 (Ellis *et al.*, 2005). Deletion of the Msc2 gene (the *msc2Δ* mutation) is reported to affect intracellular distribution of zinc ions (Li and Kaplan, 2001). The *msc2Δ* mutation aggravates ER stress that is caused by culturing cells under zinc deficient conditions (Ellis *et al.*, 2004). Conversely, depletion of cytosolic zinc ions upon zinc deficiency seems to be alleviated by the *msc2Δ* mutation, since this mutation compromises Zap1's induction (Ellis *et al.*, 2004), which results from cytosolic zinc depletion (Zhao and Eide, 1998; Bird *et al.*, 2000). Deletion of the *ZRG17* gene (the *zrg17Δ* mutation) shows phenotypes similar to that of the *msc2Δ* mutation (Ellis *et al.*, 2005). Base on these observations, it is proposed Zrg17/Msc2 heterocomplex contributes transfer of zinc ions from cytosol to the ER under zinc deficient conditions.

The insights described here have led me to pose some research questions about relationship between ER stress (and the ER-stress sensor Ire1) and zinc depletion (and the intracellular zinc transporter Zrg17). The first is the molecular mechanism by which zinc depletion causes ER stress. As aforementioned, it is possible that zinc depletion impairs protein folding in the ER. On the other hand, zinc depletion is reported to alter membrane-lipid composition (Carman and Han, 2007), possibly causing ER stress via membrane-lipid aberrancy. The second question is whether Ire1 is actually associated with Zrg17 in yeast cells. Finally, if the answer to the second question is positive, what is the functional significance of this association? In the present study, I have addressed these questions and found that Ire1 acts on Zrg17 not as an RNase but as a kinase to cope with severe zinc deficiency.

II. MATERIALS AND METHODS

2.1. Oligonucleotides

Oligonucleotides used in this study were chemically synthesized by Life Technologies Japan (Tokyo). They are listed in Tables 1 and 2.

2.2. DNA manipulation

Yeast genomic DNA was extracted by using "Dr. GenTLE (from Yeast) High Recovery" kit (Takara Bio, Otsu, Japan). For PCR from yeast genomic DNA and purified plasmids, ExTaq DNA polymerase (Takara Bio) and Pyrobest DNA polymerase (Takara Bio) were respectively employed. The procedures for the DNA extraction and PCR were based on the manufacturer's instructions. Yeast transformation was done as described in Kaiser *et al.* (1994).

2.3. Yeast plasmids

Plasmid pCZY1 is a yeast 2μ-based multicopy plasmid carrying the *URA3* selectable marker and the *E. coli* lacZ reporter gene (Mori *et al.*, 1992). On pCZY1, transcription of the lacZ gene is from the *CYC1*-core promoter that is neighbored by a promoter element upregulated by the Hac1 protein (UPR element; UPRE). Thus this plasmid was used to monitor activation of Ire1 and evocation of the UPR in yeast cells.

Plasmids pRS313 and pRS315 are yeast centromeric vectors respectively carrying the *HIS3* and the *LEU2* selectable markers (Sikorski and Hieter, 1989). Plasmids pRS313-IRE1 and pRS315-IRE1-HA are from previous studies by my current laboratory (Kimata *et al.*, 2004). To generate pRS313-IRE1, the *IRE1* gene carrying authentic 5'- and 3'-flanking sequences was cloned into the *Bam*HI/*Not*I sates of pRS313.

5

The C-terminal and 3'-flanking sequence of the *IRE1* gene was swapped to a three-tandem-copy HA-epitope sequence, and the product gene was named as *IRE1*-HA (Kimata *et al.*, 2003), which was cloned into the *Bam*HI/*Not*I sates of pRS315, generating pRS315-IRE1-HA. To generate pRS423-IRE1-HA (Kimata *et al.*, 2003), the *IRE1*-HA gene was cloned into a yeast 2μ-based multicopy vector pRS423 carrying the *HIS3* selectable marker (Christianson *et al.*, 1992). The ΔIII mutant version of pRS315-IRE1-HA was also generated previously (Promlek *et al.*, 2011).

Other mutations were introduced into the *IRE1* and the *IRE1*-HA genes on pRS313-IRE1 and pRS315-IRE1-HA by using overlap PCR and *in vivo* homologous recombination techniques (Kimata *et al.*, 2004). As the first-round PCR, the *IRE1* or the *IRE1*-HA gene was amplified with primer sets [the 1720 forward *IRE1* primer/a reverse mutation primer] and [a forward mutation primer/the PRS outer primer]. Then the two PCR products were mixed and used as a template for the second-round PCR with a primer set [the 1874 forward *IRE1* primer /the PRS inner primer], yielding a fusion of the mutated *IRE1* fragment and a partial pRS-vector sequence. The *IRE1* and the *IRE1*-HA genes used in the present study carries an artificial synonymous mutation that confers an *Xba*I-digestion site at position 1903 (Kimata *et al.*, 2004). Thus pRS313-IRE1 or pRS315-IRE1-HA was digested with *Xba*I and *Not*I, mixed with the second-round-PCR products and then used for transformation of yeast cells. The transformants were selected by histidine or leucine prototrophy, and checked for carrying the expected *IRE1* mutant gene using the genomic PCR technique.

Argon *et al.* (2009) reported that yeast Ire1 molecules carrying the green fluorescent protein (GFP)-tagging sequence at its juxtamembrane position (Ire1-GFP) is functional for evoking the UPR. For expression Ire1-GFP from the strong *TEF1* promoter, I used

pRS313-TEF1p-IRE1-GFP (Ishiwata-Kimata *et al.*, 2013).

2.4. Yeast strains

Yeast strains used in this study are listed in Table 3. They were derived from strain KMY1005 (*MATa ura3-52 leu2-3,112 his3-Δ200 trp1-Δ901 lys2-801*; Mori *et al.*, 1996).

Strain KMY1015 is an *IRE1*-gene-knockout (*ire1Δ*) variant of KMY1005 (*ire1::TRP1*; Mori *et al.*, 1996). In a previous study by my current laboratory, two UPR reporter genes, (UPRE)₅-(CYC1 core promoter)-LacZ and UPRE-(CYC1 core promoter)-GFP were introduced into the KMY1015 genome, generating strain KMY1516 (*MATa ura3-52 his3-Δ200 trp1-Δ901 LEU2::UPRE-(CYC1 core promoter)-GFP::1eu2-3,112 LYS2::(UPRE)₅-(CYC1 core promoter)-LacZ::lys2-801 ire1::TRP1*). Strain KMY1045 is an *HAC1*-gene-knockout (*hac1Δ*) variant of KMY1005 (*hac1::TRP1*; Mori *et al.*, 1996). The *URA3* gene flanked by the 5'- and 3'-UTRs of the *IRE1* gene was PCR amplified from an *ire1::URA3* strain YKY1003 (Kimata *et al.*, 2006) with a primer set [Forward *IRE1*-upstream/ Reverse *IRE1*-downstream] and introduced into the KMY1045 genome, generating an *IRE1 HAC1* double-knockout strain YNV001 (*ire1::URA3 hac1::TRP1*).

Myc-epitope tagging of the *ZRG17* gene is illustrated in Fig. 1 and was performed as follows. *Schizosaccharomyces pombe* strain art1-13myc, carrying the art1 gene tagged with 13-tandem Myc epitope at the C terminus, was provided from Dr, Kawamukai (Shimane Univ.). The C-terminal Myc-tagging module containing the *kanMX6* selectable marker, which had been originally described in Bahler *et al.* (1998) as pFA6a-13Myc-kanMX6, was PCR amplified from art1-13myc genomic DNA with primers fused with *ZRG17* (or its 3'-UTR) specific sequence (Table 2; *ZRG17*-tagging-F and *ZRG17*-tagging-C). The PCR products was

then used for transformation of KMY1516 and YNV001, yielding strains YNV002 (*ire1::TRP1 ZRG17*-MYC::*kanMX6*) and YNV003 (*ire1::URA3 hac1::TRP1 ZRG17*-MYC::*kanMX6*).

Yeast *ZRG17*-gene-knockout (*zrg17Δ*) strain Y15414 (*zrg17::kanMX4*) was provided from EUROSCARF (http://www.uni-frankfurt.de/fb15/mikro/euroscarf/index.html). The *kanMX4* sequence fused to *ZRG17* 5'- and 3'-UTR sequences was PCR amplified from Y15414 genomic DNA with a primer set [Forward *ZRG17*-upstream/Reverse *ZRG17*-downstream], and used for transformation of KMY1015 and KMY1516, yielding YNV004 (*ire1::TRP1 zrg17::kanMX4*) and YNV005 (*ire1::TRP1 zrg17::kanMX4*).

Yeast *TPK1*-gene-knockout (*tpk1Δ*) strain Y01261 (*tpk1::kanMX4*) was also provided from EUROSCARF, and transformed with a *Not*I-digested fragment of plasmid pUG72 (Gueldener *et al.*, 2002), causing replacement of *kanMX4* to *URA3* and yielding a *tpk1::URA3* strain YNV006. The *URA3* sequence fused to *TPK1* 5'- and 3'-UTR sequences was PCR amplified from YNV006 genomic DNA with a primer set [Forward *TPK1*-upstream/Reverse *TPK1*-downstream], and used for transformation of YNV002, yielding strain YNV007 (*ire1::TRP1 ZRG17*-MYC::*kanMX6 tpk1::URA3*).

2.5. Yeast culture

Culture density (OD_{600}) was measured by using Bio-Rad spectrophotometer SmartSpec 3000.

Synthetic dextrose (SD) medium contained 2% dextrose and 0.66% yeast nitrogen base without amino acids (YNB w/o AA; Becton, Dickinson and Company). Low-zinc medium (LZM) contained 2% glucose, 0.17% YNB w/o AA, 0.5% ammonium sulfate, 0.588% trisodium citrate, 1mM

EDTA, 25 μM $MnCl_2$ and 10 μM $FeCl_2$. Into SD medium and LZM, appropriate auxotrophic requirements were added at these concentrations; uracil 50 mg/L, leucine 50 mg/L, lysine 40mg/L and histidine 30 mg/L. The media were autocleaved at 120 °C for 20 min just after mixing the indicated materials. For supplementation of LZM with zinc ions, $ZnCl_2$ was dissolved into LZM to a final concentration of 100 mM, and further diluted by LZM appropriately just before usage.

Yeast cells were cultured at 30 °C with shaking in these media. For culturing in LZM in Figs 2 to 4, yeast cells were first cultured in SD medium, and the exponentially growing culture (OD_{600} 1.5-2.0) was centrifuged at 1,750 Xg for 2 min. The pellet cells were then suspended into LZM for OD_{600} to be approximately 0.5. Otherwise, in Figs 6, 7 and 9-13, pellet cells from the exponentially growing SD-medium culture were suspended into equal volume LZM supplemented with 10 μM $ZnCl_2$ and incubated for 10 hr. Then the culture was centrifuged again, and the pellet cells were re-suspended in to LZM for OD_{600} to be approximately 0.5.

2.6. β-galactosedase assay

β-galactosidase activity of cells was determined using the protocol of Kaiser *et al.* (1994). Cells (approximately 0.5 to 1.0 OD_{600} equivalent) were suspended in 800 μL of Z buffer (60 mM Na_2HPO_4, 40 mM NaH_2PO_4, 10 mM KCl, 1 mM $MgSO_4$, 0.27% 2-mercaptoethanol, pH 7.0), and 20 μL of 0.1% SDS and 50 μL of chloroform was added. The mixture was then vortexed vigorously for 20 sec. After equilibration at 28 °C for 5 min, *o*-nitrophenyl-β-D-galactoside was added to a final concentration of 0.8 mg/mL. The reaction was stopped at various times by adding 0.5 mL of 1 M Na_2CO_3, and the concentration of the product, *o-nitro*-phenol (ONP), was measured by optical density at 420 nm. One unit of β-galactosidase activity is defined as 1 nmol of ONP/min of reaction for 1 mL of culture at

9

1 OD$_{600}$ unit.

2.7. RNA analyses

DNA probes for Northern blot analysis were prepared by PCR amplification of yeast genomic DNA with primer sets shown in Table 2 (Forward *ZAP1* and Reverse *ZAP1*; Forward *ZRG17* and Reverse *ZRG17*).

The hot phenol method was used for extraction of total RNA from yeast cells. Cells (approximately 2.5 to 5.0 OD$_{600}$ equivalent) were harvested and suspended in 400 µL of the RNA extraction buffer containing 50 mM sodium acetate (pH5.3) and 10m M EDTA. After addition of 40 µL of 10% SDS and 400 µL of water-saturated 65 °C phenol, the suspension was incubated for 1 hr with occasional top-speed vortexing. Then the suspension was chilled at -80 °C for more than 1 hr, and after defrosting, centrifuged at 15,000 Xg for 10 min. Then the water fraction was subjected to phenol-chloroform extraction twice, and RNA was precipitated from the resulting water fraction by addition of 1/10-volume of 3 M sodium acetate (pH5.3) and 2.5-fold volume of ethanol. After washed with 70% ethanol and dried up, RNA was dissolved into 20 to 30 µL of water.

For Northern blot analysis, 5 µg of total RNA was separated on a 1% agarose, 1.8% formaldehyde gel and transferred to a nylon membrane (Hybond-N; GE Healthcare). The membrane was prehybridized in 500 mM sodium phosphate, pH 7.0, 1 mM EDTA, and 7% SDS. The membrane was then incubated with the random-primed ^{32}P-labeled DNA probe. After washing, the membrane was exposed to an imaging screen (BAS-MS2040; Fuji), and signal intensity was quantified using a Fuji BAS2500 image analyzer.

To check the *HAC1*-mRNA splicing, reverse transcription (RT)-PCR

was performed (Promlek *et al.*, 2011). Total RNA samples (2 µg) were used for 10 µL-scale reverse transcription reaction with the SuperScript II Reverse Transcriptase kit (Invitrogen) and the oligo dT primer (Table 1). The reaction products (2 µL) were then mixed with 1 µL each of 10 µM *HAC1* primers (Table 1), 2 µL of 2.5 mM each dNTP mix, 2.5 µL of the supplied 10X PCR buffer, 16.37 µL of water, and 0.13 µL of TAKARA Taq DNA polymerase (5 U/µL), and subjected to a 25-cycle thermal cycle reaction of 94°C for 30 sec, 54°C 30 sec, and 72°C for 60 sec. The PCR products were then run on 2% agarose gels (0.5X TBE buffer), and the ethidium bromide-stained fluorescent images were captured by a LAS-4000 Cooled CCD camera system (Fujifilm, Tokyo, Japan). The image data were then analyzed by Fujifilm ImageGauge software in order to quantify fluorescence intensity of the $HAC1_u$ and the $HAC1_i$ bands. The "*HAC1* mRNA splicing %" value was obtained form the formula $(100X(HAC1_i$ band signal$)/[(HAC1_u$ band signal$)+(HAC1_i$ band signal$)])$.

2.8. Protein analyses

For preparation of cell lysate, yeast cells (approximately 2.5 OD_{600} equivalent) were harvested and suspended in 100 µL of buffer A (50 mM Tris-Cl, pH 7.9, 5 mM EDTA, and 1% Triton X-100) supplemented by protease inhibitors (2 mM phenylmethanesulfonyl fluoride, 10 µg/mL each of pepstatin, leupeptin and aprotinin, 1/100 volume of protease inhibitor cocktail set III (EDTA-free, Merck Millipore)) and a phosphatase inhibitor cocktail (PhosSTOP, Roche Applied Science). Glass beads (0.5 mm) were then added up to the meniscus. The cells were broken by vortexing six times for 30 sec each at maximum speed. After removal of the glass beads, the cell lysates were clarified by centrifugation (15,000 Xg for 10 min).

The cell lysates equivalent to 10 µg protein were added to an equal volume of gel loading buffer containing 125 mM Tris-HCl (pH 6.8), 20% glycerol, 4% SDS, 20 mM DTT, and 0.02% bromophenol blue. Then they

were incubated at 95 °C for 2 min and fractionated on 8% SDS-PAGE gels by using the standard SDS-PAGE protocol described by Gallagher (2012). Proteins were then transferred to polyvinylidene difluoride membrane (Immobilon-P, Merck Millipore) according to the manufacturer's instruction. The blots were blocked overnight at 4 °C in Tris-buffered saline containing 0.2% Tween 20 (T-TBS) and 5% skim milk. The following day, the blots were incubated with T-TBS containing 1% skim milk and the primary antibody (12CA5 anti-HA mouse IgG (Roche Applied Science) at 0.4 μg/ml, 9E10 anti-Myc mouse IgG (Roche Applied Science) at 2 μg/mL or YOL1/34 anti-tubulin rat IgG (Accurate Chemical & Scientific) at 1/1000 dilution). Incubation was for 3 hrs at room temperature. The blots were subsequently washed four times with T-TBS at room temperature for 3 min each. The blots were next incubated with a 1:1000 dilution of horseradish peroxidase (HRP)-coupled, goat anti-mouse or anti-rat IgG antibody (Cappel for anti-mouse and Jackson ImmunoResearch for anti-rat) in T-TBS containing 1% skim milk for 1 hr at room temperature. The blots were then washed five times with T-TBS at room temperature for 3 min each, and specific protein bands were detected using enhanced chemiluminescence (ECL Western blotting detection system; GE Healthcare) and the LAS-4000 Cooled CCD camera system. To detect BiP by the Western blot analysis, rabbit anti-BiP antiserum (Tokunaga *et al.*, 1992) was used at a 1:1000 dilution, and HRP-coupled goat anti-rabbit IgG antibody (Cappel) was employed as the secondary antibody.

For immunoprecipitation experiments, the cell lysis was scaled up by starting from approximately 20 OD_{600}-equivalent cells and by using 200 μL buffer A. The cell lysates were then diluted with 800 μL buffer B (the same composition as buffer A except containing 180 mM NaCl and 6% skim milk) and incubated for 1 hr at 4 °C with 2 μg of 12CA5 mouse anti-HA antibody or 5 μL of 9B11 mouse anti-Myc antibody (Cell

Signaling Technology), followed by addition of 15 μL of protein A-conjugated Sepharose beads (Protein A Sepharose 4 FF; GE Healthcare). After further incubation at 4 °C for 1 hr, the Sepharose beads were collected by centrifugation, washed five times with buffer C (the same composition as buffer B except for containing no skim milk), and used as immunoprecipitates, which were subjected to the aforementioned Western blot analysis.

Instead of buffer A, buffer D (the same composition as buffer A except for containing no EDTA) was used to make cell lysates for Phos-tag-containing SDS-PAGE. For Phos-tag-containing SDS-PAGE to check phosphorylation status of Ire1-HA, the standard SDS-PAGE protocol described by Gallagher (2012) was employed, and 5%-polyacrylamide separating gels carried additionally 25 μM Phos-tag acrylamide (NARD Institute, Amagasaki, Japan) and 50 μM $MnCl_2$. For Phos-tag-containing SDS-PAGE to check phosphorylation status of Myc-tagged Zrg17 (Zrg17-Myc), stacking gels (4.5% acrylamide, 0.19% bisacrylamide and 350 mM bis-Tris-HCl (pH6.8)) and separating gels (7% acrylamide, 0.19% bisacrylamide, 350 mM bis-Tris-HCl (pH6.8), 6.7 μM Phos-tag acrylamide and 20 μM $ZnCl_2$) were solidified by ammonium persulfate and tetramethylethylenediamine, and running buffer contained 0.1 M Tris base, 0.1 M 3-morpholinopropanesulfonic acid, 0.1 M sodium bisulfite and 0.1% SDS.

2.9. Fluorescent microscopy

Axiophoto (Carl Zeiss MicroImaging) was used with an oil immersion lens (Plan-Neofluor 100/1.30), and images were captured by a CCD camera system (DP70; Olympus) carrying built-in software for image acquisition.

III. RESULTS

3.1. The mechanism by which zinc deficiency damages the ER

According to UPRE-lacZ reporter assay performed by Ellis *et al.* (2004), culturing yeast cells in LZM evokes the UPR. This finding suggests ER-stress induction and Ire1 activation by zinc deficiency. To confirm this insight, here I checked Ire1 activation using more direct methodologies.

In the experiment shown in Fig. 2A, splicing of the *HAC1* mRNA was monitored via RT-PCR amplification and electrophoresis fractionation of the *HAC1* species. In *IRE1+* cells (the *ire1Δ* cells strain transformed with an *IRE1* plasmid), *HAC1^u* was converted efficiently to *HAC1^i* when cells were transferred to zinc-depletion conditions (lanes 7 to 9), as is also seen upon treatment with an *N*-glycosylation inhibitor tunicamycin (lane 6), which yields aberrant proteins in the ER. As expected, the *HAC1* mRNA was not spliced in *ire1Δ* cells (lanes 1 to 3). Moreover, as shown in Fig. 1B, GFP tagged Ire1 (Ire1-GFP; Aragon *et al.*, 2009) demonstrates a diffuse distribution throughout the ER in non-stressed cells. However, stringent zinc depletion as well as tunicamycin treatment caused a punctate localization of Ire1-GFP (Figs 2C and D), which reflects higher-order oligomerization of Ire1 (Aragon *et al.*, 2009; Kimata *et al.*, 2007). We thus conclude that zinc deficiency actually causes ER stress that activates Ire1.

In order to address how zinc deficiency damages the ER and activates Ire1, I employed the ΔIII mutant version of Ire1. As reported previously (Kimata *et al.*, 2007) and reproduced in Fig. 3A, wild-type-Ire1-expressing cells exhibit sharp induction of the UPRE-lacZ

reporter upon tunicamycin treatment, which is considerably compromised by the ΔIII mutation (compare column 5 to 2 (89% reduction)). However, depletion of inositol, which is a major membrane-lipid component, induces the UPR similarly in wild-type-Ire1-expressing cells and in ΔIII-Ire1-expressing cells (Fig. 3A (compare columns 3 and 6) and Promlek et al., 2011). I then explored the case of zinc deficiency. As shown in Fig. 3B, zinc depletion activates wild-type Ire1 to a considerable level, and the ΔIII mutation only moderately compromises the UPR upon zinc depletion (compare column 15 to 11 (39% reduction)). We thus speculate that two different issues, namely ER accumulation of unfolded proteins and membrane-lipid abnormality, are induced by zinc deficiency and additively activate Ire1.

Deletion of the *ZRG17* gene has been reported to aggravate ER stress induced by zinc deficiency (Ellis *et al.*, 2005). Here we observed that the *zrg17Δ* mutation significantly enhances the level of the UPR induced by zinc deficiency in wild-type-Ire1-expressing cells (columns 13 and 11) but not in ΔIII-Ire1-expressing cells (columns 17 and 15). This finding suggests that zinc depletion from the ER, which is aggravated by the *zrg17Δ* mutation, mainly damages ER protein folding rather than membrane-lipid homeostasis. In other words, the membrane-lipid abnormality that activates ΔIII Ire1 may be caused by zinc depletion from another cellular compartment, possibly cytosol/nuclei.

When misfolded in the ER, proteins often form aggregates incorporating the ER-located molecular chaperone BiP. We are thus able to monitor protein-folding ability in the ER via measuring the cellular level of sedimentable BiP (Promlek *et al.*, 2011). In Fig. 4, cells stressed by zinc deficiency or which remained unstressed were lysed in the presence of the mild detergent Triton X-100, and fractionated by centrifugation. We then found that zinc deficiency drastically increases the amount of BiP in

the pellet fractions, suggesting impairment of protein folding in the ER.

3.2. Physical interaction between Ire1 and Zrg17

 In my present study, association between Ire1 and Zrg17 in yeast cells were confirmed using epitope-tagging and co-immunoprecipitation techniques. For tagging Zrg17 with Myc epitope, a C-terminal Myc-tagging DNA module was inserted into yeast genome as illustrated in Fig. 1, yielding Zrg17-Myc-expressing cells. Because endogenous expression level of Ire1 is reported to be low (Ghaemmaghami *et al.*, 2003), C-terminally HA-epitope-tagged Ire1 (Ire1-HA) was expressed from a 2μ plasmid (Kimata *et al.*, 2003). Cells employed here did not carry endogenous Ire1.

In the experiments shown in Fig. 5, cells were cultured in normal SD medium or stressed by DTT, and their cell lysates were subjected to anti-HA immunoprecipitation. Western-blot analysis of cell lysates (Input) indicates that as expected, anti-Myc and anti-HA antibodies respectively recognized Zrg17-Myc and Ire1-HA. Double bands of Ire1-HA are due to partial degradation of this protein (Kimata *et al.*, 2004).

The third panel of Fig. 5A indicates that anti-HA immunoprecipitation of Ire1-HA was successful. By comparing lane 6 to 4 in Fig. 5A, I noticed that Zrg17-Myc was co-immunoprecipitated with Ire1-HA. ER stress by DTT did not seem to significantly change the co-immunoprecipitation level (Fig. 5A, compare lane 1 to 4). As shown in Fig. 5B, co-immunoprecipitation between Ire1-HA and Zrg17-Myc was observed even when Ire1-HA carried the ΔIII mutation. I then assume that the association of Zrg17-Myc with Ire1-HA is not due to Ire1's ability to capture unfolded proteins, which is abolished by the ΔIII mutation (Kimata *et al.*, 2007; Promlek *et al.*, 2011).

3.3. Ire1-dependent phosphorylation and stabilization of Zrg17

According to Wu *et al.* (2011), zinc deficiency induces Zrg17 not only at the mRNA level but also at the protein level. Considering also that Ire1 is activated by zinc depletion, I hypothesized that Ire1 may contribute to the induction of Zrg17. As shown in Fig. 6, I then monitored how zinc deficiency changes cellular Zrg17 level through anti-Myc Western-blot detection of Zrg17-Myc from lysates of *IRE1+* cells. Unlike to the report by Wu *et al.* (2011), expression level of Zrg17-Myc changed unstraightforwardly in the culturing conditions employed here (Fig. 6A). First, thorough shifting cells from normal SD medium to LZM supplemented with 10 μM $ZnCl_2$ and culturing further for 10 hrs, Zrg17-Myc was decreased (Fig. 6B, compare lane 1 to 6). Second, when the resulting culture was then shifted to LZM not supplemented with $ZnCl_2$, the cellular level of Zrg17-Myc was recovered (Fig. 6B lanes 1 to 4). In my present study, I then focused on this step in which Zrg17-Myc is induced by severe zinc deficiency under the culturing condition highlighted by the yellow background in Fig. 6A.

As shown in Figs 7A and C, cells not carrying Ire1 showed compromised induction of Zrg17-Myc upon the change of culturing condition from moderate to severe zinc deficient condition. Intriguingly, *IRE1+* cells not carrying the *HAC1* gene showed a Zrg17-Myc induction similarly to the *IRE1+ HAC1+* cells (Fig. 7), though the *HAC1* mRNA is the sole already-known target of Ire1. This finding thus indicates a new function of Ire1 that is independent of *HAC1*. Consistently, the absence of Ire1 compromised the induction of Zrg17-Myc even in *hac1Δ*-background strains (Figs 7B and C).

As touched upon in the introduction section, the cytosolic domain of Ire1 has two different enzymatic activities as a Ser/Thr protein kinase and as an RNase. The aspartate at the 828th amino-acid residue of Ire1 (D828)

is within the conserved DFG kinase motif (Lee *et al.*, 2008), and reportedly, substitution of alanine on this residue (the D828A mutation; Fig. 8A) abolishes the kinase activity without abolishing Ire1's ability to splice the *HAC1* mRNA and to evoke the UPR (Chawla *et al.*, 2011). Conversely, according to Liu *et al.* (2000), an RNase-domain point mutation K1058A (Fig. 8A) abolishes Ire1's ability to evoke the UPR. As shown in Figs 8B and C, these insights were confirmed in my present study. In the experiment shown in Fig. 8B, cells expressing HA-tagged Ire1 or its mutants from single-copy plasmid were lysed and analyzed by Phos-tag-containing SDS-PAGE followed by anti-HA Western blotting. I then noticed that wild-type and K1058A Ire1-HA but not D828A Ire1 exhibited band signals corresponding to their phosphorylated versions, indicating abolishment of the kinase activity (for autophosphorylation) by the D828A mutation. Conversely, the UPRE-lacZ reporter assay shown in Fig. 8C indicated that the K1058A mutation but not the D828A mutation completely abolishes Ire1's ability to evoke the UPR.

I then employed these Ire1 mutants for checking the Zrg17-Myc induction upon the severe zinc depletion. As shown in Fig. 9, the K1058A mutant version of Ire1 functioned as well as wild-type Ire1 for the induction of Zrg17-Myc. In contrast, D828A Ire1 did not seem to work. I thus think that for the induction of Zrg17-Myc, Ire1 functions not as an RNase but as a protein kinase.

Under the zinc-depleting condition employed here, Zrg17-Myc was transcriptionally induced (Fig. 10), as its expression is governed by the authentic *ZRG17* promoter. Although this result can partly explain the induction of Zrg17-Myc at the protein level, neither loss of the *IRE1* nor the *HAC1* gene did not seem to significantly affect the Zrg17-Myc mRNA induction (Fig. 10). I thus think that Ire1 controls the cellular level of Zrg17-Myc in a post-transcriptional manner.

In the experiment shown in Fig. 11, cells were incubated in the severe zinc-deficient condition with cycloheximide, which inhibits protein synthesis. I then noticed that the cellular level of Zrg17-Myc decreased faster in cells lacking the *IRE1* gene than in *IRE1+* cells. This finding indicates that Ire1 works for stabilization of Zrg17.

Since Ire1 physically interacts with Zrg17 and functions as a protein kinase to stabilize it, I hypothesized that Zrg17 is phosphorylated in an Ire1-dependent manner. In order to check phosphorylation status of Zrg17, lysates from cells expressing Zrg17-Myc were run on Phos-tag-containing SDS-PAGE gels, which were then analysed by anti-Myc Western blotting. As shown in Fig. 12A, slow-migrating bands of Zrg17-Myc were not observed when the lysate sample was treated with a protein phosphatase before the electrophoresis, indicating that as expected, they are phosphorylated species of Zrg17-Myc. The phosphorylated species got apparent in a time dependent manner when *IRE1+* cells were shifted to the severe zinc-deficient condition (Fig. 12B lanes 2, 4 and 6). It also should be noted that Zrg17-Myc is slightly phosphorylated even in cells not carrying Ire1 (Fig. 12B lanes 1, 3 and 5). I thus think that another kinase(s) also works to phosphorylate Zrg17-Myc, though at least under this condition, the major kinase for Zrg17-Myc phosphorylation is likely to be Ire1.

3.4. Ire1 promotes Zrg17-dependent cytosol-to-ER transport of zinc ions

As described thus far, the findings from my present study indicate that under the severe zinc deficient condition, Ire1 stabilizes Zrg17. Finally, I approached a consequence of this phenomenon for physiology of yeast cells.

Zap1 acts as a sensor for cytosolic and nuclear zinc ions, and the

ZAP1 gene, which is positively controlled by Zap1 *per se*, is transcriptionally induced upon depletion of cytosolic/nuclear zinc ions (Zhao and Eide, 1997; Bird *et al.*, 2000). Here I noticed that cells carrying wild-type or K1058A Ire1 strongly induced the *ZAP1* mRNA level in response to the severe zinc deficiency (Fig. 13A, compare lane 5 to 11, and lane 4 to 10, and Fig. 13B). This induction was compromised by the absence of the *IRE1* gene (Fig. 13A, compare lane 12 to lanes 10 and 11, and Fig. 13B). Moreover, such a phenomenon was not observed in *zrg17Δ* cells (Fig. 13A lanes 7, 8 and 9, and Fig. 13B). These observations are consistent with the scenario in which Zrg17, an cytosol-to-ER zinc ion transporter, is phosphorylated and stabilized by Ire1 upon the severe zinc deficiency, depriving the cytosol and nuclei of limited zinc ions.
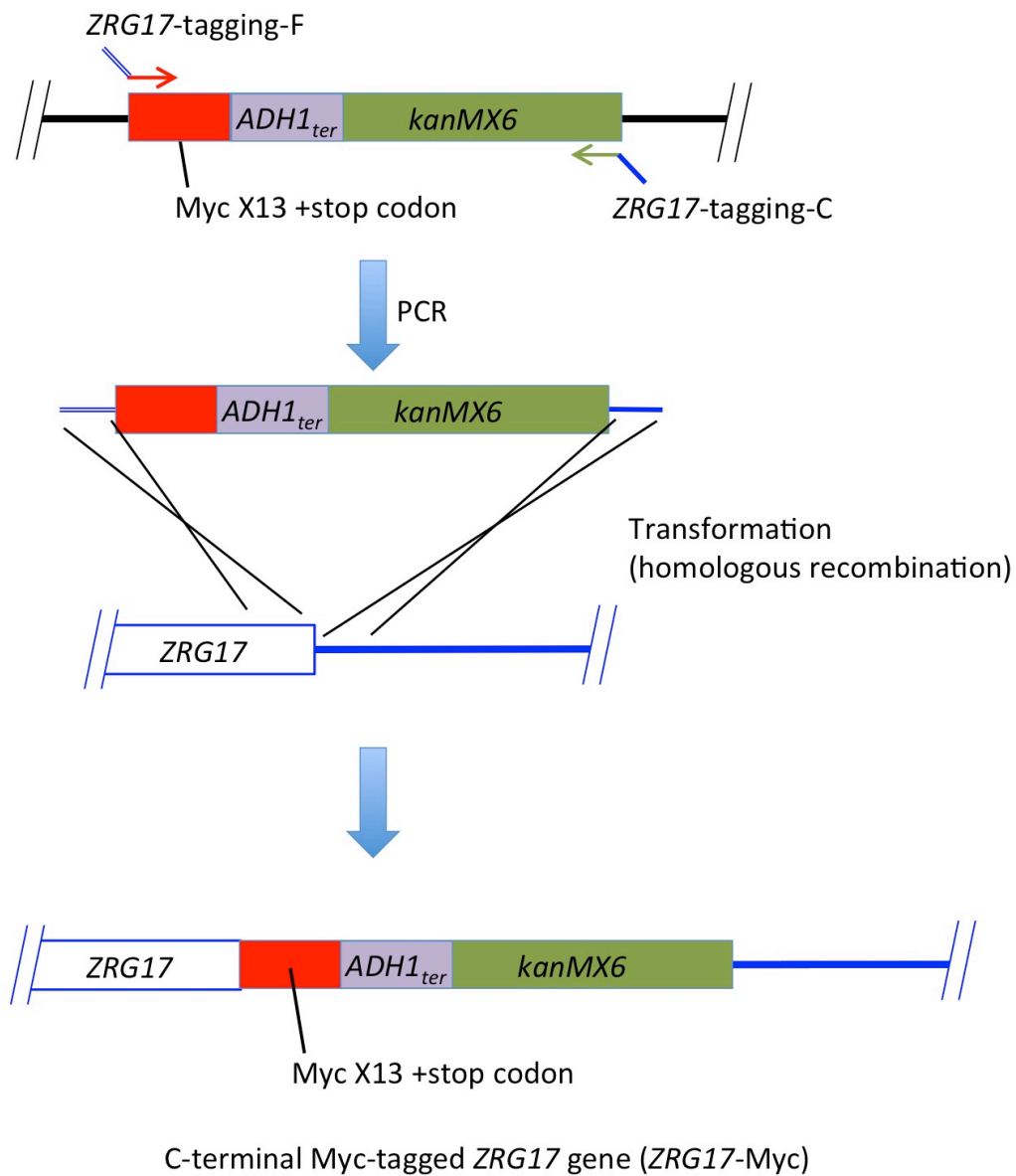
Figure 1. C-terminal epitope tagging of Zrg17.
C-terminal Myc-tagging DNA module, which is a fusion of 13-tandem copy of the Myc-epitope sequence, stop codon, *S. cerevisiae ADH1* transcriptional termination region and the *KanMX6* selectable marker, was PCR amplified using a primer set [*ZRG17*-tagging-F/*ZRG17*-tagging-C]. Because the primers carry *ZRG17*-hybridizing sequence, the PCR product is integrated into the *ZRG17* locus of *S. cerevisiae* genome through transformation of yeast cells.
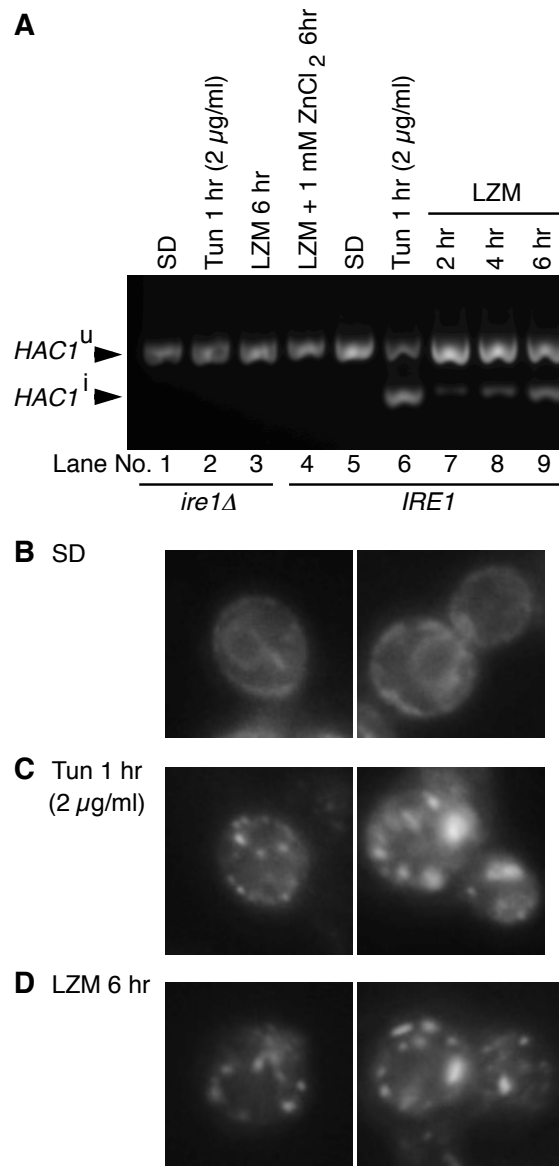
Figure 2. Ire1 activation upon zinc deficiency.

A, An *ire1Δ* strain KMY1015 carrying a centromeric *IRE1* plasmid pRS315-IRE1-HA ("*IRE1*" cells) or the empty vector pRS315 ("*ire1Δ*" cells) was cultured in SD medium (lanes 1 and 5) and then shifted to LZM (lanes 3 and 7-9). Cells were also stressed by addition of tunicamycin (Tun) to the SD medium (lanes 2 and 6) or cultured in LZM supplemented with a high-concentration (1mM) of ZnCl₂ (lane 4). The RNA samples were subjected to RT-PCR using the poly-thymine RT primer and the *HAC1*-specific PCR primers, the products of which were then run on 2% agarose. B-D, After being transformed with the Ire1-GFP expression plasmid pRS313-TEF1p-Ire1-GFP (Ishiwata-Kimata *at al.*, 2013), the *ire1Δ* strain KMY1015 was stressed by tunicamycin ("Tun"; C) or zinc depletion (D), or remained unstressed in SD medium (B). GFP fluorescence was then microscopically observed.
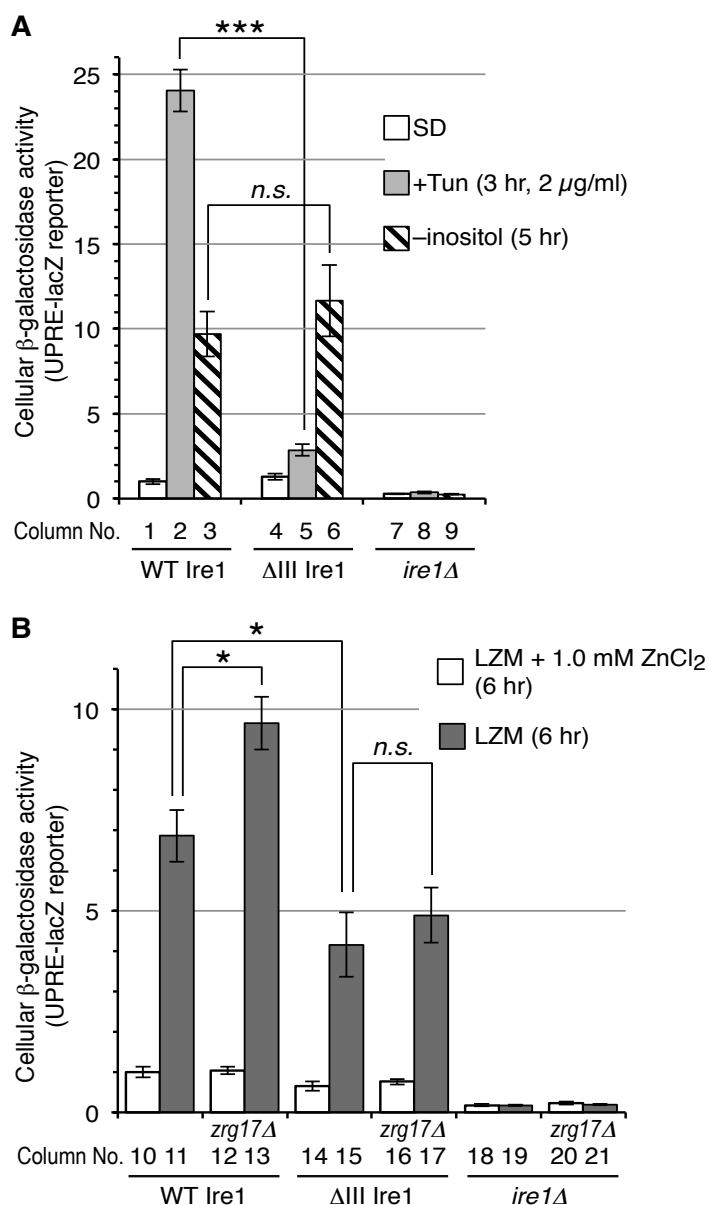
22

Figure 3. UPR induction profiles of wild-type and ΔIII-mutant versions of Ire1.

After transformation with the *IRE1* plasmid pRS315-IRE1-HA ("WT Ire1"), its ΔIII mutant version ("ΔIII Ire1") or the empty vector pRS315 ("*ire1Δ*"), the *ire1Δ* strain KMY1015 (A and B) and its *zrg17Δ* derivative YNV004 (B) carrying the UPRE-lacZ reporter plasmid pCZY1 were cultured in SD medium and treated as indicated. See Promlek *et al.* (2011) for the inositol-depletion conditions. Cellular ß-galactosidase activity was then monitored and normalized against the values of the furthest left columns set at 1.0. *, $p < 0.05$, ***, $p < 0.001$, *n.s.*, not significant.
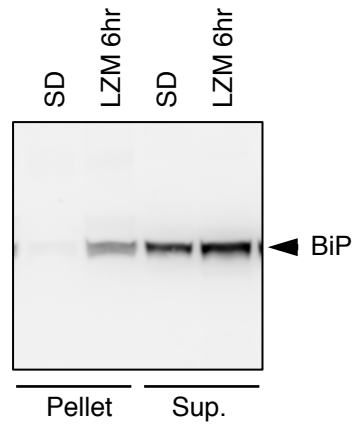
Figure 4. BiP aggregation upon zinc deficiency.

The *ire1Δ* strain KMY1015 transformed with the *IRE1* plasmid pRS315-IRE1-HA was cultured in SD medium or in LZM for 6 hrs. Total cell lysates were then fractionated by centrifugation at 8,000 x g for 20 min, and the supernatant fractions (equivalent to 0.1 OD_{600} cells) and pellet fractions (equivalent to 1.0 OD_{600} cells) were analyzed by anti-BiP Western blotting.
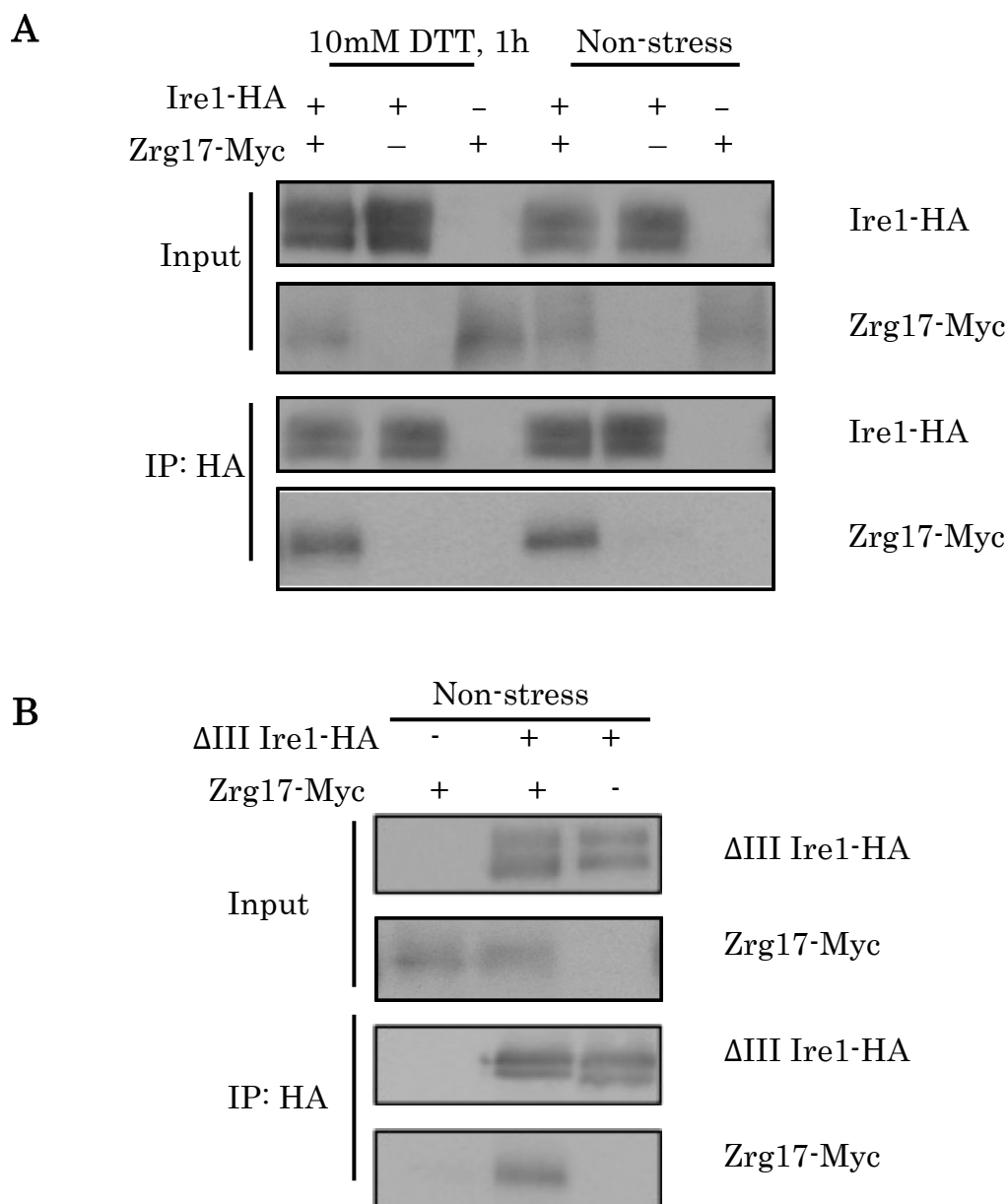
Figure 5. Ire1 interacts with Zrg17.

The Zrg17-Myc *ire1Δ* cells (YNV002; "Zrg17-Myc" [+]) or the *ire1Δ* cells with the untagged *ZRG17* gene (KMY1516; "Zrg17-Myc" [–]) carrying the 2μ wild-type Ire-HA plasmid pRS423-IRE1-HA (A; "Ire1-HA" [+]), its ΔIII mutant version (B; "ΔIII Ire1-HA" [+]) or the empty vector pRS423 ("Ire1-HA" or "ΔIII Ire1-HA" [–]) were cultured in SD medium ("Non-stress") or stressed by 10 mM DTT for 1 hr. Their cell lysates ("Input") and anti-HA immuprecipitation samples ("IP: HA") were then analysed by anti-HA or anti-Myc Western blotting.
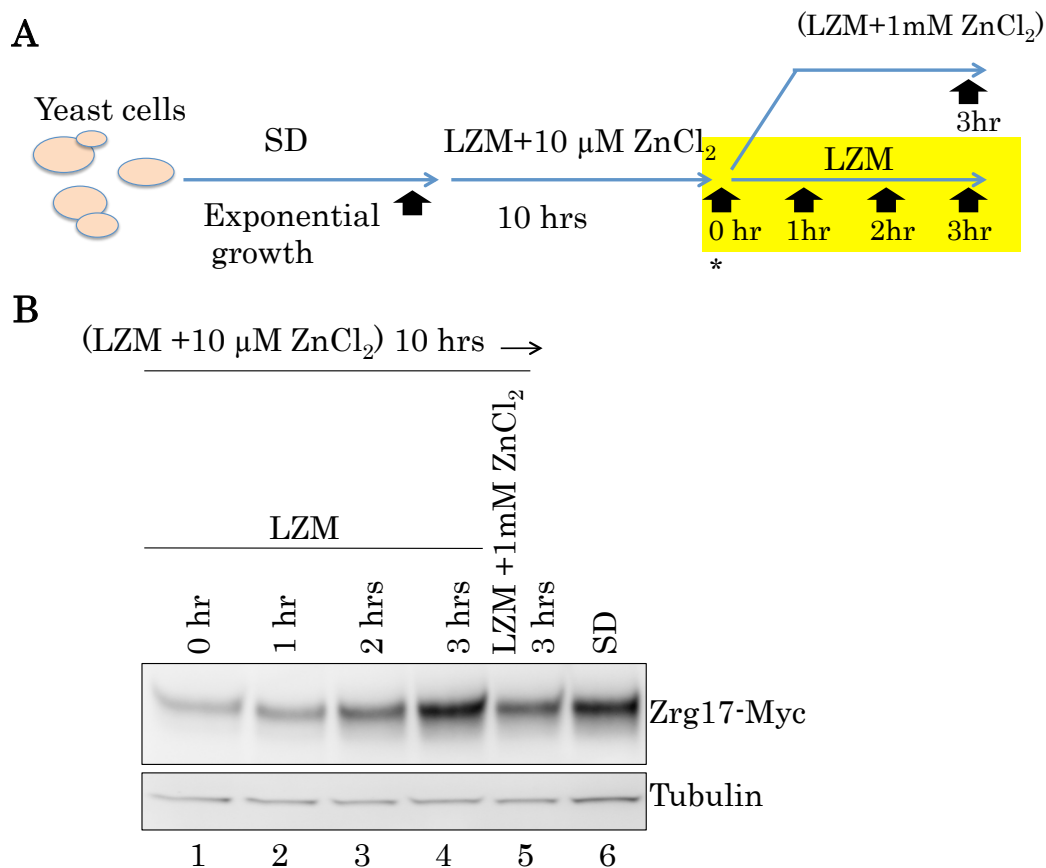
Figure 6. Change of cellular Zrg17-Myc protein level upon zinc depletion.

A, Cell culturing and harvesting procedure. Black arrows indicate sample-collection points in the experiment shown in panel B. Sample-collection duration in the experiments shown Figs 7 to 13 are highlighted by yellow background (In the experiment shown in Fig. 11, cycloheximide was added into the culture at the time-point marked by the asterisk). B, The Zrg17-Myc *ire1Δ* cells (YNV002) transformed with the *IRE1* plasmid pRS313-IRE1 were cultured in SD medium (lane 6) and then shifted to LZM supplemented with 10 μM $ZnCl_2$ for 10 hrs (lane 1). Next, the resulting culture was shifted again to LZM (lanes 2 to 4) or LZM supplemented with 1 mM $ZnCl_2$ (lane 5) for the indicated durations. The cell lysates corresponding to 10 μg total protein were then analysed by anti-Myc and anti-tubulin Western blotting.

Figure 7. Ire1 but not *HAC1* contributes to induction of Zrg17-Myc by severe zinc depletion.
A and B, After being cultured in LZM supplemented with 10 μM ZnCl₂ for 10 hrs, the Zrg17-Myc *ire1Δ* cells (A; YNV002) or the Zrg17-Myc *ire1Δhac1Δ* cells (B; YNV003) transformed with the *IRE1* plasmid pRS313-IRE1 ("*IRE1*") or the empty vector pRS313 ("*ire1Δ*") were shifted to LZM for the indicated durations. The cell lysates corresponding to 10 μg total protein were 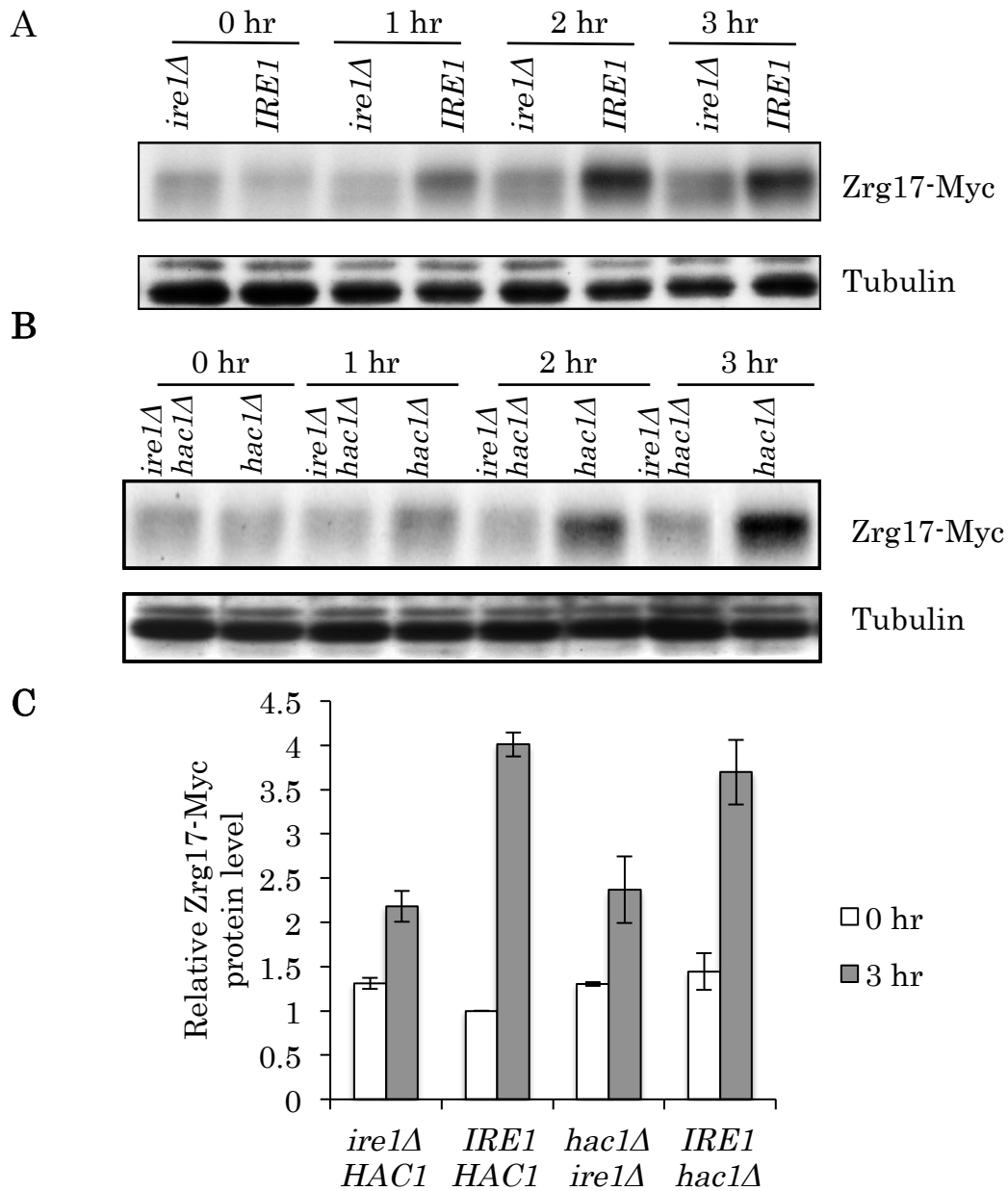then analysed by anti-Myc and anti-tubulin Western blotting. C, The same experiment as A and B was performed using three independent clones for each genotype, and protein-band density of anti-Myc Western blot was quantified and is expressed as the average and standard deviation, setting the average value from "*IRE1 HAC*1, 0 hr" samples as 1.00.

27

A Lumenal domain Cytosolic domain

Kinase RNase

D828A

K1058A

IRE1

B

| *IRE1* | K1058A | D828A | *IRE1* |

Tun   -   +   +   +

Phosphorylated
Non-phosphorylated
Ire1-HA

C

β-galactosidase assay (UPRE-lacZ reporter)

Non-stress
Tun

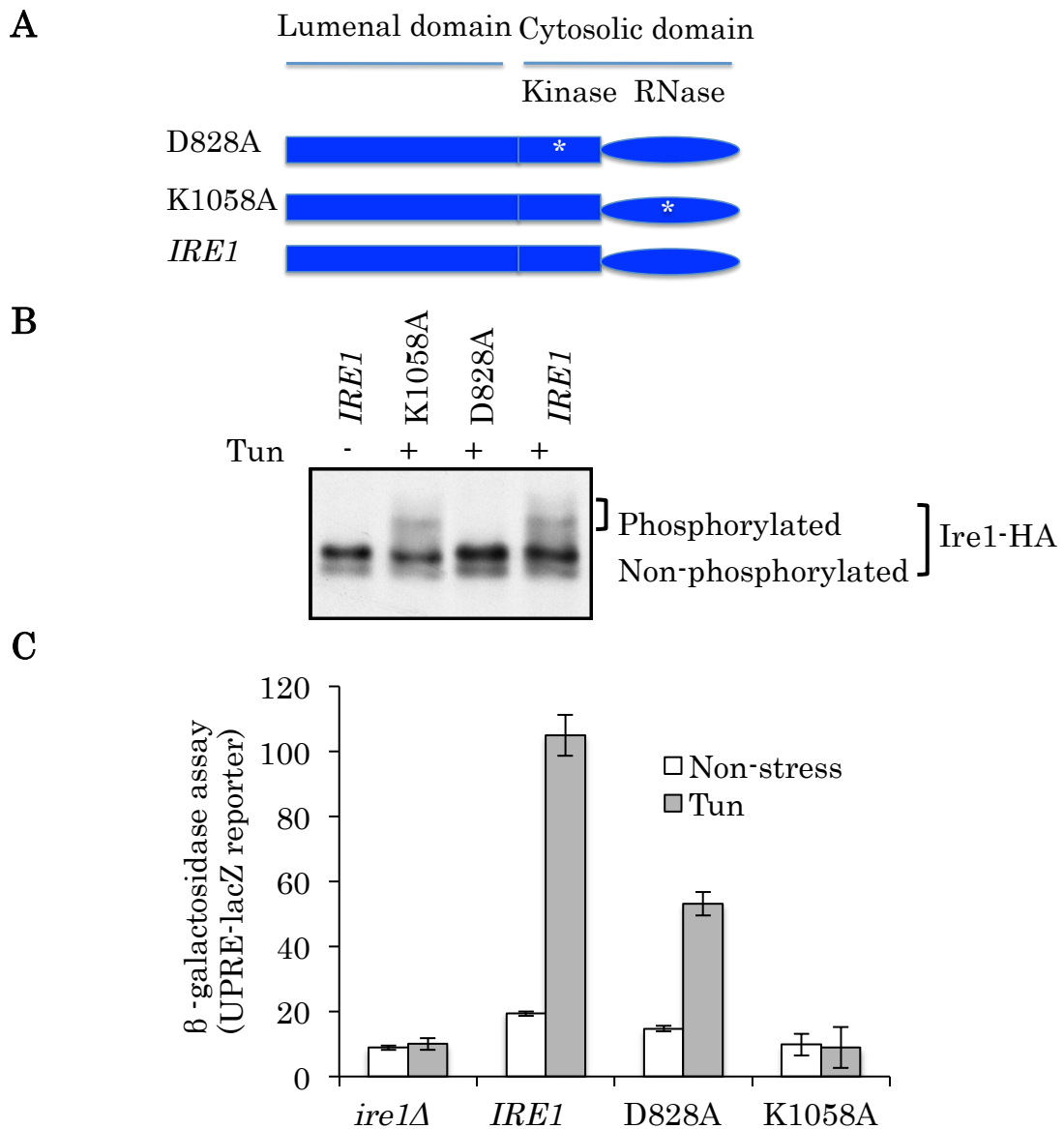ire1Δ   IRE1   D828A   K1058A

Figure 8. Cytosolic mutants of Ire1.
A, Point-mutation positions of D828A and K1058A mutants. B, The *ire1Δ*
cells (KMY1015) transformed with the IRE1-HA plasmid
pRS315-IRE1-HA (*IRE1*) or its mutants were cultured in SD medium, and
then stressed by tunicamycin ("Tun" [+]; 2 μg/mL 30 min) or unstressed
("Tun" [−]). Their lysates corresponding to 10 μg total protein were run on
Phos-tag-containing SDS-PAGE gel, which was then analysed by anti-HA
Western blotting. C, The *ire1Δ* cells (KMY1015) doubly transformed with
the UPRE-lacZ reporter plasmid pCZY1 and the IRE1-HA plasmid
pRS315-IRE1-HA (*IRE1*), its mutants or the empty vector pRS315
("*ire1Δ*") were cultured in SD medium, and then stressed by tunicamycin
("Tun"; 2 μg/mL 4 hrs) or unstressed ("Non-stress") for measuring cellular
β-galactosidase activity, which is expressed as average and standard
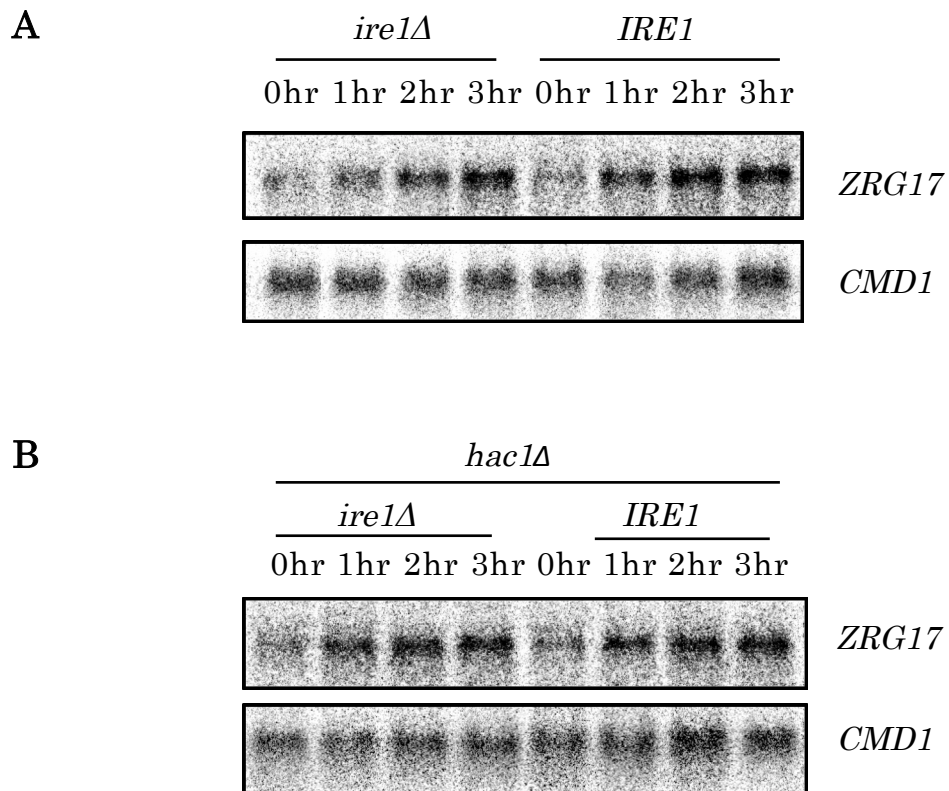deviation from three independent clones for each genotype.

Figure 9. The kinase-deficient but not the RNase-deficient mutation abolishes Ire1's ability to induce Zrg17-Myc by severe zinc depletion.

A, After being cultured in LZM supplemented with 10 μM ZnCl$_2$ for 10 hrs, the Zrg17-Myc *ire1Δ* cells (YNV002) transformed with the *IRE1* plasmid pRS313-IRE1 ("*IRE1*"), its mutants or the empty vector pRS313 ("*ire1Δ*") were shifted to LZM for the indicated durations. The cell lysates corresponding to 10 μg total protein were then analysed by anti-Myc and anti-tubulin Western blotting. B, The same experiment as A was performed using three independent clones for each genotype, and protein-band density of anti-Myc Western blot was quantified and is expressed as the average and standard deviation, setting the average value from "*IRE1*, 0 hr" samples as 1.00.

A

B

Figure 10. Transcriptional induction of Zrg17 is independent of Ire1 or *HAC1*.
Total RNA samples were extracted from the cells cultured as done in Fig. 7 were analyzed by Northern blotting using the indicated probes. The *CMD1* probe was used as a loading control.
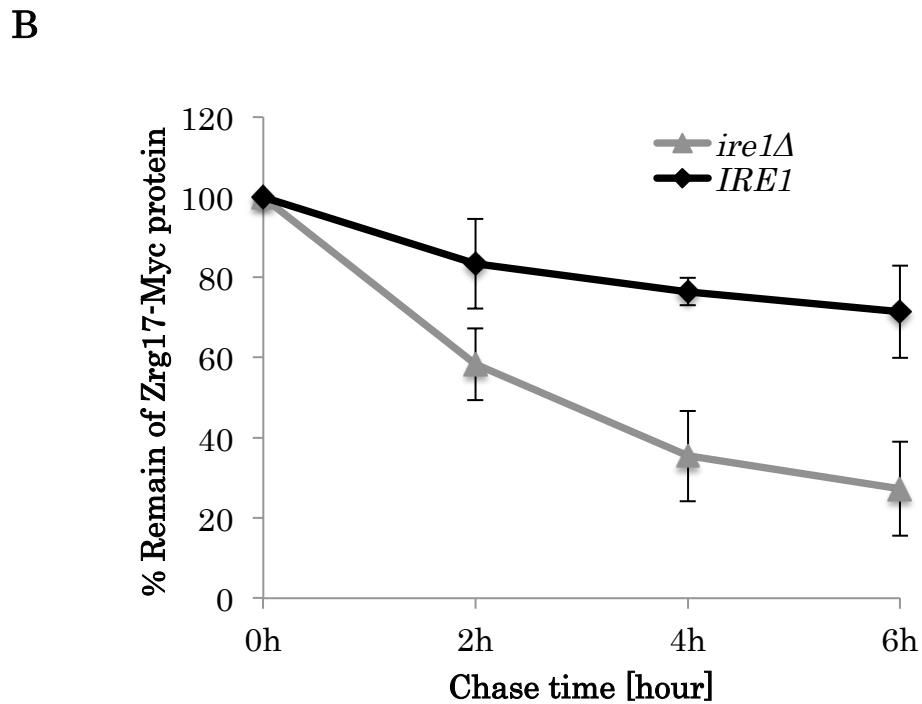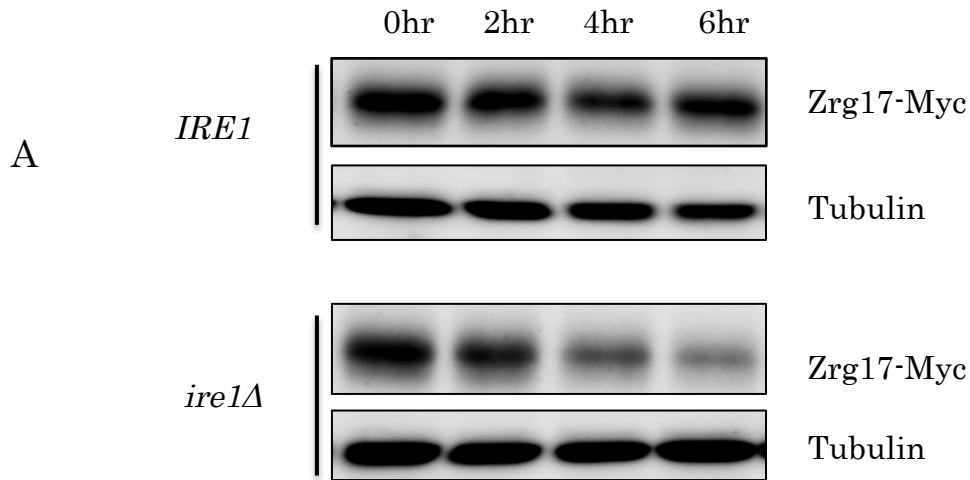
Figure 11. Cycloheximide chase indicates Ire1-depended stabilization of Zrg17-Myc under the severe-zinc deficient condition.
After being cultured in LZM supplemented with 10 μM $ZnCl_2$ for 10 hrs, the Zrg17-Myc *ire1Δ* cells (YNV002) carrying the *IRE1* plasmid pRS313-IRE1 ("*IRE1*") or the empty vector pRS313 ("*ire1Δ*") were shifted to LZM containing 250 μg/mL cycloheximide for the indicated durations. After anti-Myc Western blotting of cell lysates (corresponding 10 μg total protein), the relative amount of remaining Zrg17-Myc was quantified and is expressed as average and standard deviation form three independent clones for each genotype.
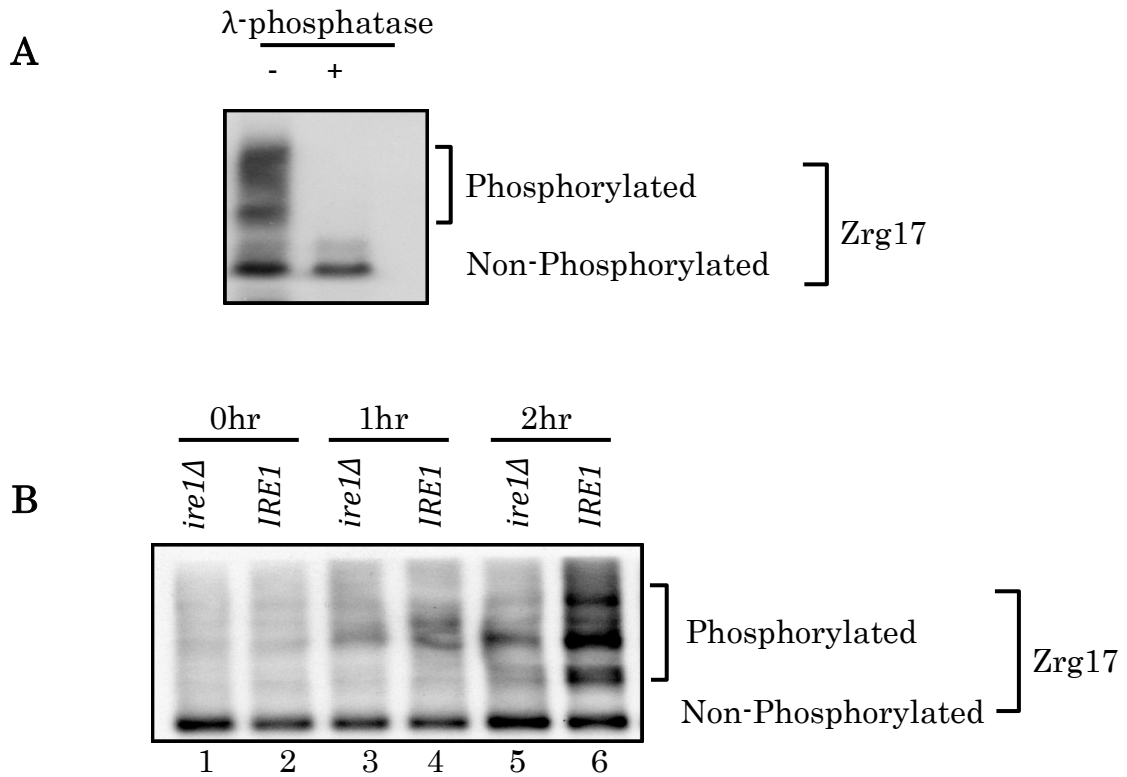
A

λ-phosphatase

B

Figure 12. Ire1-dependent phosphorylation of Zrg17-Myc.
A, After being cultured in LZM supplemented with 10 μM ZnCl$_2$ for 10 hrs, the Zrg17-Myc *ire1Δ* cells (YNV007) carrying the *IRE1* plasmid pRS313-IRE1 was shifted to LZM for 3 hrs. The cell lysate corresponding to 10 μg total protein was treated with λ-protein phosphatase ("λ-PPase" [+]) or remained untreated ("λ-PPase" [–]), and then was run on Phos-tag-containing SDS-PAGE gel, and Zrg17-Myc was detected by anti-Myc Western blotting. B, The Zrg17-Myc *ire1Δ* cells (YNV002) carrying the *IRE1* plasmid pRS313-IRE1 ("*IRE1*") or the empty vector pRS313 ("*ire1Δ*") were similarly incubated in LZM supplemented with 10 μM ZnCl$_2$ and LZM for the indicated durations, and analysed by Phos-tag-containing SDS-PAGE and anti-Myc Western blotting.

Figure 13. Ire1- and Zrg17-dependent *ZAP1* mRNA induction under the severe zinc deficient conditions.

After being cultured in LZM supplemented with 10 μM ZnCl₂ for 10 hrs, the Zrg17-Myc *ire1Δ* cells (YNV002) or *zrg17Δ ire1Δ* cells ("*zrg17Δ*"; YNV004) transformed with the *IRE1* plasmid pRS313-IRE1 ("*IRE1*"), its K1058A mutant or the empty vector pRS313 ("*ire1Δ*") were shifted to LZM for the indicated durations, and total RNA samples were analyzed by Northern blotting using the indicated probes. Band density was then quantified and is expressed as average and standard deviation from three independent clones for each genotype.
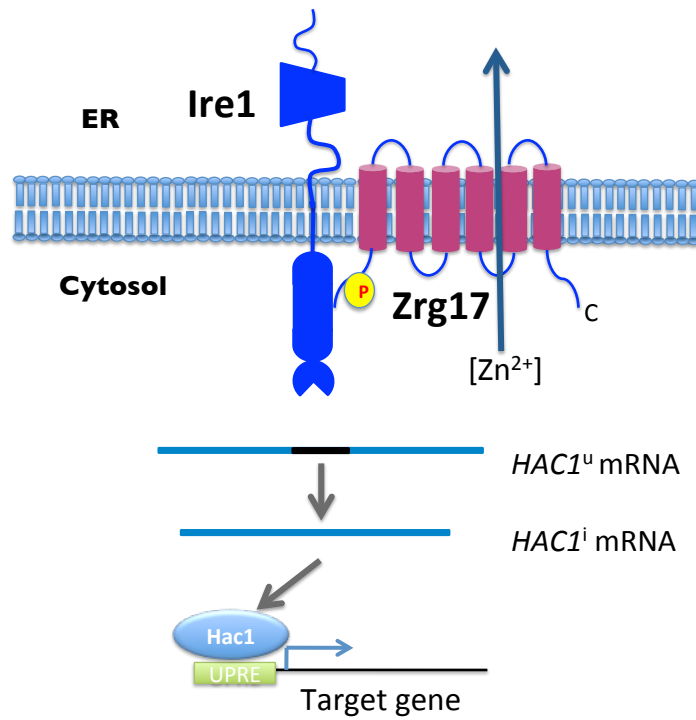
Figure 14. Current model for a new function of Ire1.
Upon severe zinc depletion, the ER is strongly damaged, activating Ire1 for phosphorylation and stabilization of Zrg17. Then, zinc ions is transported to the ER.

IV. DISCUSSION

As shown in Fig. 5, Zrg17 physically interacts with Ire1 in yeast cells. Since both Ire1 and Zrg17 are reported to be ER-located transmembrane proteins, I assume that they associate on the ER membrane. The ΔIII mutation of Ire1, which impairs interaction between Ire1 and ER-accumulated unfolded proteins, did not abolish the association of Ire1 with Zrg17. I thus think that the Ire1-Zrg17 association is not due to the Ire1's ability to capture unfolded proteins. Rather, I think that this finding implies a new molecular-biological issue concerning relationship between ER stress and intracellular zinc-ion transport.

By using the UPRE-lacZ reporter technique, Ellis *et al.* (2004) previously reported that zinc deficiency induces the UPR. Because the UPRE is also controlled by factors other than Ire1 (Leber *et al.*, 2004; Tsvetanova *et al.*, 2012), here I checked if Ire1 is actually activated by zinc depletion. As shown in Fig. 2, I then noticed that upon zinc deficiency, Ire1 is clustered and splices the *HAC1* mRNA, indicating activation of Ire1.

The present study also touches on the mechanism by which zinc deficiency leads to ER stress. According to Fig. 3B, ΔIII Ire1 was activated by zinc deficiency, but not so strong as wild-type Ire1. I thus think that zinc deficiency induces ER stress through both ER accumulation of unfolded proteins and membrane-lipid aberrancy. Recruiting BiP to sedimentable fractions (Fig. 4) strongly suggests that protein folding in the ER is damaged by zinc deficiency.

As shown in Fig. 3B, when combined with zinc deficiency, the *zrg17Δ* mutation further activates wild-type Ire1 but not ΔIII Ire1. I thus think that loss of zinc ions in the ER impairs ER protein folding rather than

membrane-lipid homeostasis. It is noteworthy that Scj1, an ER-located DnaJ-family protein that works with BiP for protein folding in the ER (Silberstein *et al.*, 1998), has putative zinc-finger motifs. Consistently, Promlek *et al.* (2011) reported that knocking-out of the *SCJ1* gene causes ER stress through impairing protein folding in the ER. In addition, zinc ions are reported to contribute to association between the ER-located thiol oxidoreductase ERp57 and lectin-type molecular chaperones (Leach *et al.*, 2002). Moreover, about one-third of proteins in the yeast proteome are deduced to traverse the ER, and I assume that like matrix metalloproteins and mammalian insulin, a significant part of them require zinc ions for proper folding. It seems thus reasonable that zinc deficiency damages protein folding in the ER. In contrast, I assume that the membrane-lipid aberrancy is due to loss of zinc ions in other cellular compartment which is probably cytosol/nuclei. According to Carman and Han (2007), Zap1 transcriptionally controls expression of some enzymes for lipid biosynthesis, causing alteration of membrane-lipid composition upon zinc depletion.

As for the mRNA level, it is widely known that Zrg17 is induced by zinc deficiency (Lyons *et al.*, 2000; Yuan *et al.*, 2000). This is due to direct interaction of the *ZRG17* promoter with Zap1 (Wu *et al.*, 2011). Since Zap1 directly senses the cytosolic/nuclear level of zinc ions (Zhao and Eide, 1997; Bird *et al.*, 2000), I assume that Zrg17 is transcriptionally induced in response to decrease of the cytosolic/nuclear zinc-ion level.

Nevertheless, as shown in Fig. 6, change of the Zrg17 protein level was not so straightforward. One issue that has not been deeply addressed in my present study is that the protein level of Zrg17 is rather high in cells cultured in normal SD medium. According to Phos-tag-containing SDS-PAGE performed preliminary in my current laboratory, Zrg17 is highly phosphorylated both in *IRE1+* cells and in *ire1Δ* cells cultured in

normal SD media. I thus assume that in healthy conditions with sufficient zinc ions, Zrg17 is stabilized through its phosphorylation by kinases other than Ire1, which may include Tpk1. It is obscure what is the physiological merit of keeping high Zrg17-protein level under normal conditions. I speculate that at least, there is no substantial disadvantage to do so for cells.

However, the cellular level of Zrg17 was decreased when cells were shifted to LZM containing 10 µM $ZnCl_2$ and further cultured for 10 hrs (Fig. 6). I further shifted the resulting culture to LZM not containing $ZnCl_2$, causing increment of the cellular Zrg17 level (Fig. 6). The main topic of my present study is the molecular and cellular biological issues underlying the induction of Zrg17 under this condition.

I assume that two different issues are responsible for the increment of the cellular level of Zrg17 under this severely zinc-deficient condition. One is the transcriptional induction in which Ire1 is not involved (Fig. 10). This is probably due to upregulation of the cytosolic/nuclear zinc-ion sensor Zap1, since autonomous induction of Zap1 was also observed under this condition (Fig. 13).

On the other hand, here I demonstrated that Ire1 is also involved in the Zrg17 induction under severe zinc deficiency. This is not a transcriptional regulation, since the Zrg17 mRNA was equally induced in *IRE1+* cells and in *ire1Δ* cells (Fig. 10). Rather, according to the cycloheximide-chase experiment shown in Fig. 11, Zrg17 was more stable in *IRE1+* cells than in *ire1Δ* cells under this condition. I thus assume that severe zinc depletion activates Ire1, which then stabilizes Zrg17.

As mention on in the introduction section, it is widely accepted that Ire1 works on its downstream molecules as an RNase. In other words, the kinase part of Ire1 has been thought to work merely for activation of its

RNase part. To my knowledge, one exception is the mammalian major Ire1 paralogue, IRE1α, which forms a complex with TRAF1 and ASK1 to activate JNK for ER stress-dependent apoptosis (Urano *et al.*, 2000; Nishitoh *et al.*, 2002). In this case, IRE1α may act as kinase, since according to Urano *et al.* (2000), an RNase-moiety-deleted mutant of IRE1α functioned to evoke apoptosis through this signaling pathway. However, this story is still somewhat obscure, since, for example, the phosphorylation target of IRE1α has not been uncovered. As described in the next two paragraphs, my present study illustrates more clearly a function of Ire1 as a kinase through proposing that yeast Ire1 phosphorylates Zrg17 for its stabilization.

The sole already-known job of yeast Ire1 is to splice the *HAC1* mRNA, the product of which evokes the UPR. However, the *hac1Δ* mutation poorly compromised the induction of Zrg17 (Fig. 7). Thus Ire1 functions to Zrg17 in a previously unknown manner, which is independent of the UPR. Being consistent with this insight, the *ire1Δ* mutation is reported to retard cellular growth more badly than the *hac1Δ* mutation under zinc-deficient conditions (North *et al.*, 2012).

Moreover, an RNase-deficient mutant but not a kinase-deficient mutant of Ire1 functioned to induce Zrg17 as well as wild-type Ire1 (Fig. 9). I thus think that Ire1 works on Zrg17 as a kinase. Indeed, Phos-tag-containing SDS PAGE shown in Fig. 12 indicated that Ire1-dependent phosphorylation of Ire1.

Considering the physical interaction between Ire1 and Zrg17, I assume that Ire1 directly phosphorylates Zrg17. In order to support this idea, it would be meaningful to check *in vitro* phosphorylation of the recombinant Zrg17 fragment by the recombinant cytosolic fragment of Ire1. The recombinant cytosolic fragment of Ire1 having kinase activity at

least for autophosphorylation was already prepared by Korennykh *et al.* (2009) using an *E. coli* recombinant-protein-expression system. As for the phosphorylation target in the *in vitro* study, I will first use a recombinant fragment of the N-terminal cytosolic segment of Zrg17, which has a number of the Ser and Thr residues that according to a computer prediction (NetPhos 2.0; http://www.cbs.dtu.dk/services/NetPhos/) are highly probably phosphorylated by Ser/Thr protein kinases.

Another possible experiment that will support my proposition is about Zrg17 mutations by which the possible phosphorylation-target Ser and/or Thr residues are replaced to other amino acids. Ser-to-Ala and Thr-to-Ala mutations will inhibit the phosphorylation, probably leading to destabilization of Zrg17. Conversely, Ser-to-Asp and Thr-to-Asp mutations may mimic phosphorylated status of Zrg17, and may stabilize Zrg17 even without Ire1.

Taken together, here I propose that multiple cellular events control cellular level of Zrg17. In yeast cells cultured in normal SD medium containing sufficient amount of zinc ions, unidentified kinases phosphorylate and stabilize Zrg17. It is obscure how Zrg17 functions under this condition. When cells are shifted to a moderately zinc-deficient condition, Zrg17 is destabilized, and the cellular level of Zrg17 is decreased. However, Zrg17 is induced in response to further shifting of cells to a severe zinc-deficient condition. I assume that this is due to both the transcriptional induction by Zap1 and the Ire1-dependent stabilization. Namely, severe zinc deficiency causes ER stress partly through impairment of protein folding in the ER, activating Ire1 not only for the UPR but also for the phosphorylation and stabilization of Zrg17 (Fig. 14).

As mentioned above, the *ZAP1* gene is transcriptionally induced in an autonomous manner (Zhao and Eide, 1997; Bird *et al.*, 2000), allowing

me to monitor depletion of cytosolic zinc ions through checking the *ZAP1*-mRNA level. According to this methodology, severe zinc depletion leads to considerable loss of cytosolic zinc ions dependently on both Ire1 and Zrg17 (Fig. 13). In this case, Ire1 works not as the UPR inducer but as a kinase for phosphorylation and stabilization of Zrg17, since the RNase-deficient mutant Ire1 functioned as well as wild-type Ire1. It is thus likely that Zrg17 is stabilized by Ire1 upon severe zinc deficiency promotes transport of zinc ion from cytosol to the ER.

As a conclusion, I propose the following story. Under moderate zinc deficient conditions, Zrg17 is poorly phosphorylated, causing its destabilization. In this case, the ER is not so severely damaged, and Zrg17-dependent cytosol-to-ER zinc-ion transport is not required. Rather, the limited amount of zinc ions is maintained in cytosol and the nuclei. However, upon severe zinc deficiency, the ER is strongly damaged, activating Ire1 for stabilization of Zrg17. Then, the limited amount of zinc ions is transported to the ER. This scenario is an intriguing example for which a limited amount of a cellular component is properly distributed between different cellular compartments.

V. ACKNOWLEDGEMENT

VI. REFERENCES

Aragon, T., van Anken, E., Pincus, D., Serafimova, I. M., Korennykh, A. V., Rubio, C. A., and Walter, P. (2009). Messenger RNA targeting to endoplasmic reticulum stress signalling sites. Nature *457*, 736-740.

Bahler, J., Wu, J. Q., Longtine, M. S., Shah, N. G., McKenzie, A., 3rd, Steever, A. B., Wach, A., Philippsen, P., and Pringle, J. R. (1998). Heterologous modules for efficient and versatile PCR-based gene targeting in Schizosaccharomyces pombe. Yeast *14*, 943-951.

Bird, A. J., Zhao, H., Luo, H., Jensen, L. T., Srinivasan, C., Evans-Galea, M., Winge, D. R., and Eide, D. J. (2000). A dual role for zinc fingers in both DNA binding and zinc sensing by the Zap1 transcriptional activator. EMBO J. *19*, 3704-3713.

Calfon, M., Zeng, H., Urano, F., Till, J. H., Hubbard, S. R., Harding, H. P., Clark, S. G., and Ron, D. (2002). IRE1 couples endoplasmic reticulum load to secretory capacity by processing the XBP-1 mRNA. Nature *415*, 92-96.

Carman, G. M., and Han, G. S. (2007). Regulation of phospholipid synthesis in Saccharomyces cerevisiae by zinc depletion. Biochim. Biophys. Acta. *1771*, 322-330.

Chawla, A., Chakrabarti, S., Ghosh, G., and Niwa, M. (2011). Attenuation of yeast UPR is essential for survival and is mediated by IRE1 kinase. J. Cell Biol. *193*, 41-50.

Christianson, T. W., Sikorski, R. S., Dante, M., Shero, J. H., and Hieter, P. (1992). Multifunctional yeast high-copy-number shuttle vectors. Gene *110*, 119-122.

Cox, J. S., and Walter, P. (1996). A novel mechanism for regulating activity of a transcription factor that controls the unfolded protein response. Cell *87*, 391-404.

Credle, J. J., Finer-Moore, J. S., Papa, F. R., Stroud, R. M., and Walter, P. (2005). On the mechanism of sensing unfolded protein in the endoplasmic reticulum. Proc. Natl. Acad. Sci. USA *102*, 18773-18784.

Eide, D. J. (2006). Zinc transporters and the cellular trafficking of zinc. Biochim. Biophys. Acta. *1763*, 711-722.

Ellis, C. D., Macdiarmid, C. W., and Eide, D. J. (2005). Heteromeric protein complexes mediate zinc transport into the secretory pathway of eukaryotic cells. J. Biol. Chem. *280*, 28811-28818.

Ellis, C. D., Wang, F., MacDiarmid, C. W., Clark, S., Lyons, T., and Eide, D. J. (2004). Zinc and the Msc2 zinc transporter protein are required for endoplasmic reticulum function. J. Cell Biol. *166*, 325-335.

Gallagher, S. R. (2012). One-dimensional SDS gel electrophoresis of proteins. Curr. Protoc. Mol. Biol. *Chapter 10*, Unit 10 12A.

Gardner, B. M., and Walter, P. (2011). Unfolded proteins are Ire1-activating ligands that directly induce the unfolded protein response. Science *333*, 1891-1894.

Ghaemmaghami, S., Huh, W. K., Bower, K., Howson, R. W., Belle, A., Dephoure, N., O'Shea, E. K., and Weissman, J. S. (2003). Global analysis of protein expression in yeast. Nature *425,* 737-741.

Gueldener, U., Heinisch, J., Koehler, G. J., Voss, D., and Hegemann, J. H. (2002). A second set of loxP marker cassettes for Cre-mediated multiple gene knockouts in budding yeast. Nucleic Acids Res. *30*, e23.

Han, D., Lerner, A. G., Vande Walle, L., Upton, J. P., Xu, W., Hagen, A., Backes, B. J., Oakes, S. A., and Papa, F. R. (2009). IRE1alpha kinase activation modes control alternate endoribonuclease outputs to determine divergent cell fates. Cell *138*, 562-575.

Hollien, J., Lin, J. H., Li, H., Stevens, N., Walter, P., and Weissman, J. S. (2009). Regulated Ire1-dependent decay of messenger RNAs in mammalian cells. J. Cell Biol. *186*, 323-331.

Hollien, J., and Weissman, J. S. (2006). Decay of endoplasmic reticulum-localized mRNAs during the unfolded protein response. Science *313*, 104-107.

Ishiwata-Kimata, Y., Yamamoto, Y. H., Takizawa, K., Kohno, K., and Kimata, Y. (2013). F-actin and a type-II myosin are required for efficient clustering of the ER stress sensor Ire1. Cell Struct. Funct. *In press.*

Kaiser, C., Michaelis, S., and Mitchell, A. (1994). Methods in Yeast Genetics: A Cold Spring Harbor Laboratory Course Manual. Cold Spring Harbor, NY: Cold Spring Harbor Laboratory Press.

Kimata, Y., Ishiwata-Kimata, Y., Ito, T., Hirata, A., Suzuki, T., Oikawa, D., Takeuchi, M., and Kohno, K. (2007). Two regulatory steps of ER-stress sensor Ire1 involving its cluster formation and interaction with unfolded proteins. J. Cell Biol. *179*, 75-86.

Kimata, Y., Ishiwata-Kimata, Y., Yamada, S., and Kohno, K. (2006). Yeast unfolded protein response pathway regulates expression of genes for anti-oxidative stress and for cell surface proteins. Genes Cells *11*, 59-69.

Kimata, Y., Kimata, Y. I., Shimizu, Y., Abe, H., Farcasanu, I. C., Takeuchi, M., Rose, M. D., and Kohno, K. (2003). Genetic evidence for a role of

BiP/Kar2 that regulates Ire1 in response to accumulation of unfolded proteins. Mol. Biol. Cell *14*, 2559-2569.

Kimata, Y., Oikawa, D., Shimizu, Y., Ishiwata-Kimata, Y., and Kohno, K. (2004). A role for BiP as an adjustor for the endoplasmic reticulum stress-sensing protein Ire1. J. Cell Biol. *167*, 445-456.

Korennykh, A. V., Egea, P. F., Korostelev, A. A., Finer-Moore, J., Zhang, C., Shokat, K. M., Stroud, R. M., and Walter, P. (2009). The unfolded protein response signals through high-order assembly of Ire1. Nature *457*, 687-693.

Leach, M. R., Cohen-Doyle, M. F., Thomas, D. Y., and Williams, D. B. (2004). Localization of the lectin, ERp57 binding, and polypeptide binding sites of calnexin and calreticulin. J. Biol. Chem. *277*, 29686-29697.

Leber, J. H., Bernales, S., and Walter, P. (2004). IRE1-independent gain control of the unfolded protein response. PLoS Biol. *2*, E235.

Lee, K. P., Dey, M., Neculai, D., Cao, C., Dever, T. E., and Sicheri, F. (2008). Structure of the dual enzyme Ire1 reveals the basis for catalysis and regulation in nonconventional RNA splicing. Cell *132*, 89-100.

Li, H., Korennykh, A. V., Behrman, S. L., and Walter, P. (2010). Mammalian endoplasmic reticulum stress sensor IRE1 signals by dynamic clustering. Proc. Natl. Acad. Sci. USA *107*, 16113-16118.

Li, L., and Kaplan, J. (2001). The yeast gene MSC2, a member of the cation diffusion facilitator family, affects the cellular distribution of zinc. J. Biol. Chem. *276*, 5036-5043.

Liu, C. Y., Schroder, M., and Kaufman, R. J. (2000). Ligand-independent dimerization activates the stress response kinases IRE1 and PERK in the lumen of the endoplasmic reticulum. J. Biol. Chem. *275*, 24881-24885.

Lyons, T. J., Gasch, A. P., Gaither, L. A., Botstein, D., Brown, P. O., and Eide, D. J. (2000). Genome-wide characterization of the Zap1p zinc-responsive regulon in yeast. Proc. Natl. Acad. Sci. USA *97*, 7957-7962.

Mori, K. (2009). Signalling pathways in the unfolded protein response: development from yeast to mammals. J. Biochem. *146*, 743-750.

Mori, K., Kawahara, T., Yoshida, H., Yanagi, H., and Yura, T. (1996). Signalling from endoplasmic reticulum to nucleus: transcription factor with a basic-leucine zipper motif is required for the unfolded protein-response pathway. Genes Cells *1*, 803-817.

Mori, K., Ma, W., Gething, M. J., and Sambrook, J. (1993). A transmembrane protein with a cdc2+/CDC28-related kinase activity is required for signaling from the ER to the nucleus. Cell *74*, 743-756.

Mori, K., Sant, A., Kohno, K., Normington, K., Gething, M. J., and Sambrook, J. F. (1992). A 22 bp cis-acting element is necessary and sufficient for the induction of the yeast KAR2 (BiP) gene by unfolded proteins. EMBO J. *11*, 2583-2593.

Nishitoh, H., Matsuzawa, A., Tobiume, K., Saegusa, K., Takeda, K., Inoue, K., Hori, S., Kakizuka, A., and Ichijo, H. (2002). ASK1 is essential for endoplasmic reticulum stress-induced neuronal cell death triggered by expanded polyglutamine repeats. Genes Dev. *16*, 1345-1355.

North, M., Steffen, J., Loguinov, A. V., Zimmerman, G. R., Vulpe, C. D., and Eide, D. J. (2012). Genome-wide functional profiling identifies genes and processes important for zinc-limited growth of Saccharomyces cerevisiae. PLoS Genet. *8*, e1002699.

Papa, F. R., Zhang, C., Shokat, K., and Walter, P. (2003). Bypassing a kinase activity with an ATP-competitive drug. Science *302*, 1533-1537.

Promlek, T., Ishiwata-Kimata, Y., Shido, M., Sakuramoto, M., Kohno, K., and Kimata, Y. (2011). Membrane aberrancy and unfolded proteins activate the endoplasmic reticulum stress sensor Ire1 in different ways. Mol. Biol. Cell *22*, 3520-3532.

Ron, D., and Walter, P. (2007). Signal integration in the endoplasmic reticulum unfolded protein response. Nat. Rev. Mol. Cell Biol. *8*, 519-529.

Rubio, C., Pincus, D., Korennykh, A., Schuck, S., El-Samad, H., and Walter, P. (2011). Homeostatic adaptation to endoplasmic reticulum stress depends on Ire1 kinase activity. J. Cell Biol. *193*, 171-184.

Shamu, C. E., and Walter, P. (1996). Oligomerization and phosphorylation of the Ire1p kinase during intracellular signaling from the endoplasmic reticulum to the nucleus. EMBO J. *15*, 3028-3039.

Sidrauski, C., and Walter, P. (1997). The transmembrane kinase Ire1p is a site-specific endonuclease that initiates mRNA splicing in the unfolded protein response. Cell *90*, 1031-1039.

Sikorski, R. S., and Hieter, P. (1989). A system of shuttle vectors and yeast host strains designed for efficient manipulation of DNA in Saccharomyces cerevisiae. Genetics *122*, 19-27.

Silberstein, S., Schlenstedt, G., Silver, P. A., and Gilmore, R. (1998). A role for the DnaJ homologue Scj1p in protein folding in the yeast endoplasmic reticulum. J Cell Biol *143*, 921-933.

Tokunaga, M., Kawamura, A., and Kohno, K. (1992). Purification and characterization of BiP/Kar2 protein from Saccharomyces cerevisiae. J. Biol. Chem. *267*, 17553-17559.

Travers, K. J., Patil, C. K., Wodicka, L., Lockhart, D. J., Weissman, J. S., and Walter, P. (2000). Functional and genomic analyses reveal an essential coordination between the unfolded protein response and ER-associated degradation. Cell *101*, 249-258.

Tsvetanova, N. G., Riordan, D. P., and Brown, P. O. (2012). The yeast Rab GTPase Ypt1 modulates unfolded protein response dynamics by regulating the stability of HAC1 RNA. PLoS Genet. *8*, e1002862.

Urano, F., Wang, X., Bertolotti, A., Zhang, Y., Chung, P., Harding, H. P., and Ron, D. (2000). Coupling of stress in the ER to activation of JNK protein kinases by transmembrane protein kinase IRE1. Science *287*, 664-666.

Volmer, R., van der Ploeg, K., and Ron, D. (2013). Membrane lipid saturation activates endoplasmic reticulum unfolded protein response transducers through their transmembrane domains. Proc. Natl. Acad. Sci. USA *110*, 4628-4633.

Wu, Y. H., Frey, A. G., and Eide, D. J. (2011). Transcriptional regulation of the Zrg17 zinc transporter of the yeast secretory pathway. Biochem. J. *435*, 259-266.

Yoshida, H., Matsui, T., Yamamoto, A., Okada, T., and Mori, K. (2001). XBP1 mRNA is induced by ATF6 and spliced by IRE1 in response to ER stress to produce a highly active transcription factor. Cell *107*, 881-891.

Yuan, D. S. (2000). Zinc-regulated genes in Saccharomyces cerevisiae revealed by transposon tagging. Genetics *156*, 45-58.

Zhao, H., and Eide, D. J. (1997). Zap1p, a metalloregulatory protein involved in zinc-responsive transcriptional regulation in Saccharomyces cerevisiae. Mol. Cell. Biol. *17*, 5044-5052.

Table 1. Oligonucleotides used in this study

Name	Sequence	Hybridizing to	Usage
1720 forward *IRE1* (alias Xba–300)	TGCCTGAAAAGGAAATCCCCATAG	*IRE1* CDS	
1874 forward *IRE1* (alias Xba–100)	CGATGATGCTGATGAAGATGATGA	*IRE1* CDS	
pRS outer (alias Not+300)	AGGAAGGGAAGAAAGCGAAAGGAG	pRS vector	
pRS inner (alias Not+50)	ACGTTGTAAAACGACGGCCAGTGA	pRS vector	
K1058A-F	GAGCACTTAGGAATGCATATCATCAT	Mutation primer	Ire1 mutation K1058A
K1058A-C	ATGATGATATGCATTCCTAAGTGCTC	Mutation primer	Ire1 mutation K1058A
D828A-F	AATTTTGATATCAGCCTTTGGTCTTTGCAA	Mutation primer	Ire1 mutation D828A
D828A-C	TTGCAAAGACCAAAGGCTGATATCAAAATT	Mutation primer	Ire1 mutation D828A
oligo dT	TTTTTTTTTTTTTTTTTTTT	mRNA	RT PCR
Forward *HAC1*	TACAGGGATTTCCAGAGCACG	*HAC1* CDS	RT PCR
Reverse *HAC1*	TGAAGTGATGAAGAAATCATTCAATTC	*HAC1* CDS	RT PCR
Forward *IRE1*-upstresm	TGCCTGAAAAGGAAATCCCCATAG	*IRE1* 5'-UTR	
Reverse *IRE1*-downstream	AGGAAGGGAAGAAAGCGAAAGGAG	*IRE1* 3'-UTR	

Table 2. Oligonucleotides used in this study

Forward *ZAP1*	GAGATTGATTGCGATTTGACCTGT	*ZAP1* CDS	Making *ZAP1* probe
Reverse *ZAP1*	CCATAGGGTGTTTGAAATCTTGAG	*ZAP1* CDS	Making *ZAP1* probe
Forward *ZRG17*	ATGGAGACGCCGCAAATGAAC	*ZRG17* CDS	Making *ZRG17* probe
Reverse *ZRG17*	TTATATTCGGTCTATGTCTATTG	*ZRG17* CDS	Making *ZRG17* probe
ZRG17-tagging-F	ACGAGCATTCCAACGTGTGAAACTACA ATAGACATAGACCGAATATCGTACGCT GCAGGTCGA		Myc tagging of Zrg17
ZRG17-tagging-C	TAGTAATATTAATATGTATGTATTGAT GGGTATGTAACTGTAAAAATCGATGAA TTCGAGCTCGTTTA		Myc tagging of Zrg17
Forward *ZRG17*-upstresm	GATTAGCTGCGCTAGTGTGA	*ZRG17* 5'-UTR	
Reverse *ZRG17*-downstream	CGATATCATGTCCCGTGGTA	*ZRG17* 3'-UTR	
Forward *TPK1*-upstresm	AGTTTGACATAATAATCAAGGGGG	*TPK1* 5'-UTR	
Reverse *TPK1*-downstream	GGTTTATACCAAGGGGCTCACG	*TPK1* 3'-UTR	

Table 3. Strains used in this study

Name	Description	Parent	Source
KMY1005	*MATa ura3-52 leu2-3,112 his3-D200 trp1-D901 lys2-801*		Ref. 1
KMY1015	*ire1::TRP1*	KMY1005	Ref. 1
KMY1516	*ire1::TRP1* Genomic UPRE-lacZ and UPRE-GFP reporters	KMY1015	Ref. 2
KMY1045	*hac1::TRP1*	KMY1005	Ref.1
YNV001	*hac1::TRP1 ire1::URA3*	KMY1045	This study
YNV002	*ire1::TRP1 ZRG17-MYC::kanMX6* Genomic UPRE-lacZ and UPRE-GFP reporters	KMY1516	This study
YNV003	*hac1::TRP1 ire1::URA3* *ZRG17-MYC::kanMX6*	YNV001	This study
YNV004	*ire1::TRP1 zrg17::kanMX4*	KMY1015	This study
YNV005	*ire1::TRP1 zrg17::kanMX4* Genomic UPRE-lacZ and UPRE-GFP reporters	KMY1516	This study
YNV007	*ire1::TRP1 ZRG17-MYC::kanMX6 tpk1::URA3* Genomic UPRE-lacZ and UPRE-GFP reporters	YNV002	This study

Strains used only as sources of gene-disruption or gene-modification DNA modules are not listed in this table.